

The effect of upwelling on the distribution and stable isotope composition of *Globigerina bulloides* and *Globigerinoides ruber* (planktic foraminifera) in modern surface waters of the NW Arabian Sea

Frank J.C. Peeters^{a,b,*}, Geert-Jan A. Brummer^a, Gerald Ganssen^b

^aDepartment of Marine Chemistry and Geology (MCG), Netherlands Institute for Sea Research (NIOZ), P.O. Box 59, 1790 AB Den Burg, Texel, The Netherlands

^bDepartment of Paleoclimatology and Paleoecology, Faculty of Earth Sciences, Free University, De Boelelaan 1085, 1081 HV, Amsterdam, The Netherlands

Received 1 September 2000; received in revised form 19 November 2001; accepted 19 November 2001

Abstract

Hydrographic changes in the NW Arabian Sea are mainly controlled by the monsoon system. This results in a strong seasonal and vertical gradient in surface water properties, such as temperature, nutrients, carbonate chemistry and the isotopic composition of dissolved inorganic carbon ($\delta^{13}\text{C}_{\text{DIC}}$). Living specimens of the planktic foraminifer species *Globigerina bulloides* and *Globigerinoides ruber*, were collected using depth stratified plankton tows during the SW monsoon upwelling period in August 1992 and the NE monsoon non-upwelling period in March 1993. We compare their distribution and the stable isotope composition to the seawater properties of the two contrasting monsoon seasons. The oxygen isotope composition of the shells ($\delta^{18}\text{O}_{\text{shell}}$) and vertical shell concentration profiles indicate that the depth habitat for both species is shallower during upwelling (SW monsoon period) than during non-upwelling (NE monsoon period). The calcification temperatures suggest that most of the calcite is precipitated at a depth level just below the deep chlorophyll maximum (DCM), however above the main thermocline. Consequently, the average calcification temperature of *G. ruber* and *G. bulloides* is lower than the sea surface temperature by 1.7 ± 0.8 and 1.3 ± 0.9 °C, respectively. The carbon isotope composition of the shells ($\delta^{13}\text{C}_{\text{shell}}$) of both species differs from the in situ $\delta^{13}\text{C}_{\text{DIC}}$ found at the calcification depths of the specimens. The observed offset between the $\delta^{13}\text{C}_{\text{shell}}$ and the ambient $\delta^{13}\text{C}_{\text{DIC}}$ results from (1) metabolic/ontogenetic effects, (2) the carbonate chemistry of the seawater and, for symbiotic *G. ruber*, (3) the possible effect of symbionts or symbiont activity. Ontogenetic effects produce size trends in $\Delta\delta^{13}\text{C}_{\text{shell-DIC}}$ and $\Delta\delta^{18}\text{O}_{\text{shell-w}}$: large shells of *G. bulloides* (250–355 µm) are 0.33 ‰ ($\delta^{13}\text{C}$) and 0.23 ‰ ($\delta^{18}\text{O}$) higher compared to smaller ones (150–250 µm). For *G. ruber*, this is 0.39 ‰ ($\delta^{13}\text{C}$) and 0.17 ‰ ($\delta^{18}\text{O}$). Our field study shows that the $\delta^{13}\text{C}_{\text{shell}}$ decreases as a result of lower $\delta^{13}\text{C}_{\text{DIC}}$ values in upwelled waters, while the effects of the carbonate system and/or temperature act in an opposite direction and increase the $\delta^{13}\text{C}_{\text{shell}}$ as a result lower $[\text{CO}_3^{2-}]$ (or pH) values and/or lower temperature. The $\Delta\delta^{13}\text{C}_{\text{shell-DIC}}$ $[\text{CO}_3^{2-}]$ slopes from our field data are close to those reported literature from laboratory culture experiments. Since seawater carbonate chemistry affects the $\delta^{13}\text{C}_{\text{shell}}$ in an opposite sense,

* Corresponding author.

E-mail address: peef@geo.vu.nl (F.J.C. Peeters).

and often with a larger magnitude, than the change related to productivity (i.e. $\delta^{13}\text{C}_{\text{DIC}}$), higher $\delta^{13}\text{C}_{\text{shell}}$ values may be expected during periods of upwelling.

© 2002 Elsevier Science B.V. All rights reserved.

Keywords: planktic foraminifera; stable isotopes; Arabian Sea; upwelling; monsoon; carbonate system

1. Introduction

1.1. A field study

The oxygen and carbon isotope composition in shells of planktic foraminifera ($\delta^{18}\text{O}_{\text{shell}}$, $\delta^{13}\text{C}_{\text{shell}}$) provide an important tool in paleoceanographic studies as indicators of environmental changes in past surface water conditions. In order to use the stable isotope composition of the shells as a reliable paleoceanographic proxy for seawater temperature, salinity, nutrient levels, $\delta^{18}\text{O}_{\text{w}}$ or the $\delta^{13}\text{C}$ of dissolved inorganic carbon ($\delta^{13}\text{C}_{\text{DIC}}$), it is fundamental to know whether foraminifera precipitate their calcite shells in equilibrium with the ambient seawater or have predictable offsets. Previous studies have shown that the interpretation of the stable isotope composition of foraminiferal shells in upwelling areas is difficult, and often hampered by the dynamic character of such settings (Kroon and Ganssen, 1989; Curry et al., 1992; Thunell and Sautter, 1992). Although the $\delta^{18}\text{O}_{\text{shell}}$ values generally follow the temperature changes of surface waters, the $\delta^{13}\text{C}_{\text{shell}}$ was often found to be in disequilibrium with the $\delta^{13}\text{C}_{\text{DIC}}$ (e.g. Williams et al., 1977; Spero and Williams, 1988; Spero, 1992; Kohfeld et al., 1996; Mulitza et al., 1999). Because the $\delta^{13}\text{C}_{\text{shell}}$ is assumed to vary primarily with $\delta^{13}\text{C}_{\text{DIC}}$ (Spero, 1992), offsets were explained by ecological factors such as depth habitat or timing of shell growth within an upwelling cycle. In addition, different biological and kinetic processes related to food source, respiration activity and symbiont photosynthesis may affect the $\delta^{13}\text{C}_{\text{shell}}$ (Williams et al., 1977, 1981; Kahn, 1979; Deuser et al., 1981; Duplessy et al., 1981; Erez and Honjo, 1981; Kahn and Williams, 1981; Spero and Williams, 1988; Kroon and Ganssen, 1989; Bijma and Hemleben, 1994; Hemleben and Bijma, 1994; Spero and Lea, 1996). For example, Kroon and Ganssen (1989) found that, during upwelling, the

$\delta^{13}\text{C}$ of shells of *Globigerina bulloides* in the Arabian Sea were enriched in ^{13}C , while the ^{13}C depleted upwelled waters would dictate a shift in the opposite direction.

Recent culture experiments, however, suggest that the carbon isotope disequilibrium may result from the effects of the carbonate chemistry of seawater (Spero et al., 1997; Bijma et al., 1999). Their laboratory experiments with cultured non-symbiotic *G. bulloides* and symbiotic *Orbulina universa* indicate that both $\Delta\delta^{13}\text{C}_{\text{shell-DIC}}$ and $\Delta\delta^{18}\text{O}_{\text{shell-w}}$ decrease with increasing carbonate ion concentration or pH. We suggest that this mechanism may explain the enigmatic stable isotope composition of planktic foraminifera in upwelling areas such as the northern Arabian Sea (Kroon and Ganssen, 1989; Kroon et al., 1990; Curry et al., 1992; Steens et al., 1992). This area is characterized by large spatial and temporal changes in surface water hydrography and surface water carbonate chemistry (Körtzinger et al., 1997; Goyet et al., 1999). In this paper, we test to what extent the seasonal changes in surface water conditions affect the stable isotope composition in shells of living planktic foraminifera. We focus on living *G. bulloides* and *Globigerinoides ruber* collected with plankton nets in the upwelling area off Yemen/Oman in the NW Arabian Sea during two monsoon seasons (Fig. 1). We compare their depth distribution and stable isotope composition to the in situ measured environmental parameters of the upper water column. Because of their widespread distribution in the world oceans, these species are widely used as indicators of environmental changes in surface water conditions and, in particular, for paleoceanographic reconstructions of upwelling intensity and monsoon system variability (Prell and Curry, 1981; Kroon et al., 1990; Brock et al., 1992; Curry et al., 1992; Steens et al., 1992; Anderson and Prell, 1993; Naidu and Malmgren, 1995, 1996a,b; Gupta and Mohan, 1996; Ivanova, 2000; Vénec-Peyré and

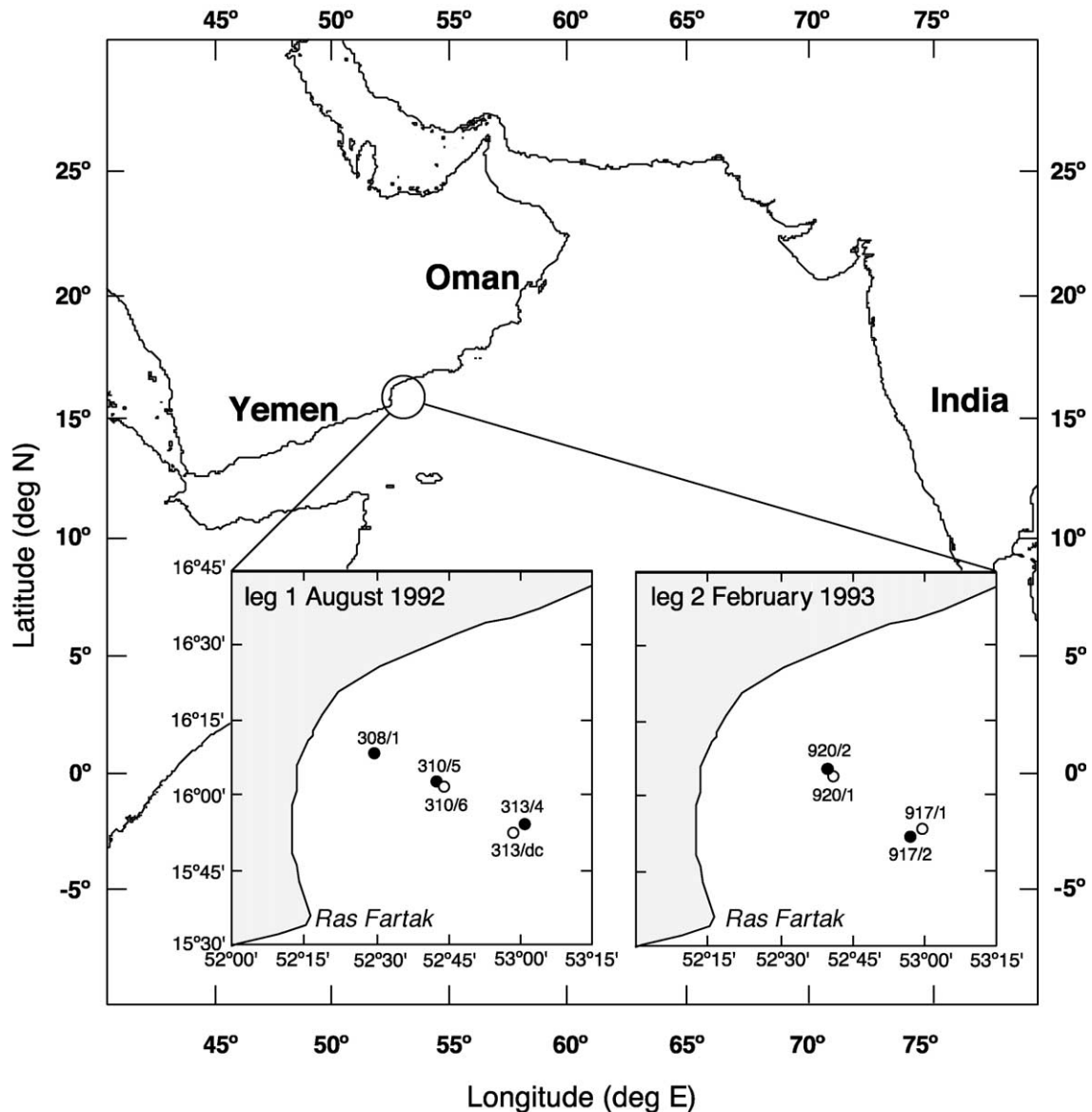


Fig. 1. Map of the Western Arabian Sea, showing locations of multi-net casts taken during C1 cruise of RV *Tyro*, in August 1992 and C2 cruise in February 1993. Closed circles indicate shallow casts (100–0 m) and open circles indicate deep casts (500–0 m). Note that the same locations have different station numbers; stations 313 and 310 are identical to 917 and 920.

Caulet, 2000). *G. bulloides* is often used as an indicator for cold and nutrient-rich upwelled waters during the SW monsoon, while *G. ruber* proliferates in warmer and oligotrophic waters during both the upwelling and non-upwelling season (e.g. Conan and Brummer, 2000). The strong seasonal contrast in

seawater temperature, carbonate chemistry and water column stratification in the NW Arabian Sea area, provides the opportunity to study the sensitivity of the stable isotope composition of planktic foraminiferal shells in relation to large seasonal changes in surface water conditions.

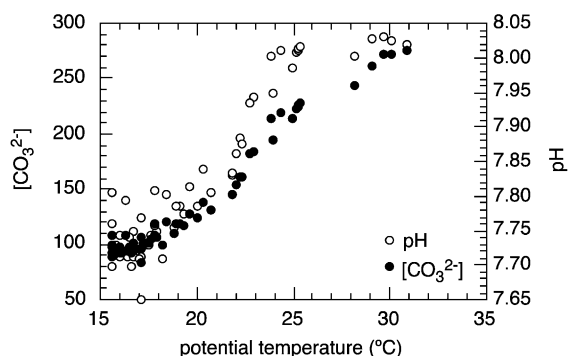


Fig. 2. The carbonate ion concentration and pH plotted vs. seawater temperature. The carbonate ion concentration and pH of upwelled waters is much lower than that of surface waters (i.e. >25 °C). Upwelling therefore may create a large seasonal gradient in surface water carbonate chemistry.

1.2. Upwelling in the Arabian Sea

Driven by the monsoon system, the sea surface hydrography in the northwestern Arabian Sea is characterized by a large seasonal gradient in surface water temperature, nutrients and biological productivity (e.g. Wyrski, 1971, 1988; McCreary et al., 1996). During summer (June to September) coastal upwelling occurs as a result of the strong SW monsoon winds, while the weaker NE monsoon winds (December–March) result in a deeply stratified ocean. During the SW monsoon upwelling period, cold and nutrient rich waters from a depth of approximately 200 m reach the sea surface, resulting in high surface water nutrient concentrations (nitrate, reactive phosphorus and dissolved silica), SSTs down to 18–22 °C and a near surface chlorophyll maximum. During the winter NE monsoon, the stratified surface waters are nutrient depleted at SSTs of 26–27 °C. The deep chlorophyll maximum, usually associated with the base of the mixed layer, is then found between 30 and 60 m. In

addition, seasonal upwelling also causes large changes in surface water carbonate chemistry. For example, upwelling in the northern Arabian Sea may lower the SST from 25 to 18 °C and bring down the carbonate ion concentration in surface waters by approximately $110 \mu\text{mol kg}^{-1}$ (Fig. 2). At the same time, the change in the ambient $\delta^{13}\text{C}_{\text{DIC}}$ is about -1 ‰. Based on the results of laboratory culture experiments (Spero et al., 1997; Bemis et al., 2000), these effects would, for example, increase the $\delta^{13}\text{C}$ of *G. bulloides* by about 0.97 ‰ to 1.11 ‰.

2. Material and methods

2.1. Sample collection

During the C cruises of the RV *Tylo*, within the framework of the Netherlands Indian Ocean Programme (NIOP) (Van Hinte et al., 1995), depth stratified plankton tows were collected along a transect perpendicular to the coast of Yemen/Oman in August 1992 (leg C1) and in February 1993 (leg C2) (Fig. 1). A modified Hydrobios Multinet system with flow meter was equipped with five plankton nets (mesh size 100 μm) and towed behind the ship. The nets were opened at depth and closed consecutively during the upcast. At the same stations sampled for planktic foraminifera, a CTD-rosette sampler was deployed for in situ measurements on temperature, salinity, inorganic nutrients and the isotopic composition of sea water (Table 1). Our data represent observations at five hydrographic stations (Fig. 1, Table 1 and 2): three of them (stations 308, 310 and 313) were sampled during SW monsoon upwelling conditions in August 1992, while the other two (stations 920 and 917) represent the NE monsoon non-upwelling conditions of February 1993 (Brummer, 1995; Peeters, 2000). Note that

Table 1
CTD stations and general hydrographic information

Station–cast	Date	Longitude	Latitude	SST (°C)	MLD (m)	DCM (m)	Remarks
308–2	8/19/92	52°30.8'E	16°08.4'N	20.49	5	5	upwelling, SW monsoon
310–1	8/20/92	52°41.7'E	16°04.0'N	20.68	6	7	upwelling, SW monsoon
313–2	8/22/92	53°00.6'E	15°52.7'N	25.75	10	9	upwelling gyre, SW monsoon
917–1	2/25/93	53°00.4'E	15°43.1'N	25.80	15	29	non-upwelling, NE monsoon
920–1	2/27/93	52°42.2'E	16°04.0'N	25.52	45	40	non-upwelling, NE monsoon

SST = sea surface temperature. MLD = mixed layer depth. DCM = deep chlorophyll maximum.

the same locations have different station numbers: stations 313 and 310 are identical to 917 and 920, respectively. The upper water column was sampled at five standard depth intervals: 100–75, 75–50, 50–25, 25–10 and 10–0 m. During both expeditions, an additional deep cast was taken at two stations (310–920 and 313–917) to a depth of 500 m, covering the intervals 500–300, 300–200, 200–150, 150–100 and 100–0 m. The shallowest net of the deep cast thus covered the entire shallow casts and therefore has not been studied. To avoid the effect of clogging, varying amounts of seawater were filtered depending on the expected amount of particulate matter. For the deep casts characteristically 100–500 m³ of seawater was filtered per interval, for shallow casts generally 20–100 m³ per interval (Table 1). Samples were stored in a borax-buffered formalin–seawater solution (pH>8.0), in 500-ml LDPE bottles, kept under dark and cool conditions and checked for their pH. For further details, see Brummer (1995).

2.2. Sample preparation

The plankton samples were frozen in liquid nitrogen using pre-weighed aluminum cups and freeze dried. The organic matter has been removed using a Low Temperature Asher. The ashed residue was sieved, using tap water, over mesh sizes of 500, 355, 250, 150 and 125 μm . After rinsing with ethanol, the size fractions were dried on a hot plate at 75 °C for approximately 45 min. We analysed the five fractions for their foraminiferal content, counting at least 200 specimens per fraction (Peeters, 2000). Planktic foraminifera were identified using a WILD M5A binocular microscope following the taxonomy of Bé (1967) and Hemleben et al. (1989). Faunal data are discussed in Peeters and Brummer (in press).

2.3. Stable isotope analysis

Whole shells of *G. bulloides* and *G. ruber* were hand picked from the size fractions 150–250 and 250–355 μm . Approximately 30–70 μg of sample was used per analysis. This corresponds to 13–30 and 10–20 *G. bulloides* shells for the 150–250 and the 250–355 μm size fraction, respectively. For *G. ruber*, 14–22 and 6–12 shells were picked from these size fractions. The

stable isotope composition of the shells was measured on a Finnigan 251 gas-source mass spectrometer, equipped with an automated carbonate extraction line. All analyses were performed at the Institute of Earth Sciences of the Free University in Amsterdam, the Netherlands. Samples have been dissolved in concentrated orthophosphoric acid at a temperature of 80 °C. Results are given relative to the Vienna Pee Dee belemnite standard (V-PDB). Calibration to the V-PDB standard was performed via NBS-18, NBS-19 and NBS-20 international standards (Hut, 1987; Coplen et al., 1983). The external reproducibility for $\delta^{18}\text{O}$ is $\pm 0.09\text{‰}$ (1 S.D.) and $\pm 0.05\text{‰}$ for $\delta^{13}\text{C}$.

2.4. Oxygen isotopes

In order to calculate the calcification temperature from the oxygen isotope composition of a foraminiferal shell, a relationship between $\delta^{18}\text{O}_{\text{shell}}$, the $\delta^{18}\text{O}$ of seawater ($\delta^{18}\text{O}_{\text{w}}$) and temperature, known as “a temperature equation”, is needed. Many temperature equations for biogenic calcite have been constructed in the past decades (e.g. Epstein et al., 1953; Craig, 1965; Horibe and Oba, 1972; Shackleton, 1974). Most of these temperature equations are close to one another but often yield calcification temperatures for living plankton which are 1–2 °C too high with respect to the ambient seawater temperature (Williams et al., 1981; Bemis et al., 1998). This has led to the construction of temperature equations for different species (Erez and Luz, 1983; Bouvier-Soumagnac and Duplessy, 1985; Bemis et al., 1998; Peeters, 2000). Two reasons may be given why different temperature equations can be found in literature. First, results from laboratory culture experiments show that, due to an ontogenetic effect, small shells are depleted in ^{18}O compared to larger ones (Spero and Lea, 1996; Bemis et al., 1998). Consequently, one needs different temperature equations for different shell sizes. In shells of *G. bulloides*, for example, the $\delta^{18}\text{O}_{\text{shell}}$ difference between the 13 and 11-chambered shells is between 0.46 ‰ (at 15 °C) and 0.12 ‰ (at 24 °C) (Bemis et al., 1998). Second, Spero et al. (1997) have shown that $\Delta\delta^{18}\text{O}_{\text{shell-w}}$ values decrease with increasing carbonate ion concentration (or pH) with a slope of $-0.004\text{‰}(\mu\text{mol kg}^{-1})^{-1}$ for *G. bulloides* and $-0.0022\text{‰}(\mu\text{mol kg}^{-1})^{-1}$ for *G. ruber* (Bijma et al., 1998). According to Zeebe (1999), this effect may

be explained by changes in the abundance of the carbonate species as a function of pH.

Given that temperature equations based on biogenic calcite may include a species specific vital effect (e.g. Niebler et al., 1999), we have chosen to define “the vital effect” ($\delta^{18}\text{O}_{\text{ve}}$) relative to the equilibrium value of inorganically precipitated calcite (Kim and O’Neil, 1997). Since inorganically precipitated calcite is free of any biological effects, offsets in the $\delta^{18}\text{O}_{\text{shell}}$ from their equilibrium value ($\delta^{18}\text{O}_{\text{eq. inorg., V-PDB}}$) must be attributed to biological factors and carbonate system effects, and as such correctly defines the term “vital effect”:

$$\delta^{18}\text{O}_{\text{VE}} = \delta^{18}\text{O}_{\text{shell}} - \delta^{18}\text{O}_{\text{eq. inorg., V-PDB}} \quad (1)$$

By substituting the equation of Kim and O’Neil (1997) into Eq. (1), the expected equilibrium value for foraminiferal calcite ($\delta^{18}\text{O}_{\text{shell}}$) can be calculated using:

$$\delta^{18}\text{O}_{\text{shell}} = [25.778 - 3.333(43.704 + T)^{0.5}] + \delta^{18}\text{O}_{\text{w}} + \delta^{18}\text{O}_{\text{ve}} \quad (2)$$

In this equation $\delta^{18}\text{O}_{\text{ve}}$ represents a species and/or size specific correction factor related to ontogenetic and carbonate system effects on the $\delta^{18}\text{O}_{\text{shell}}$. At temperatures between 15 and 24 °C, the $\delta^{18}\text{O}_{\text{shell-w}}/T$ slope of the Kim and O’Neil (1997) equation, if approximated by a linear regression, is similar to the one published by Bemis et al. (1998) for *G. bulloides*, i.e. $-0.21 \text{‰ } ^\circ\text{C}^{-1}$ (Fig. 3). If, for example, a vital effect of -0.52‰ is used in Eq. (2), the calculated equilibrium values are, within measurement errors, identical to the ones calculated from the equation for 13-chambered *G. bulloides* of Bemis et al. (1998) (Fig. 3). Depending on the species and size fraction considered, different values for $\delta^{18}\text{O}_{\text{ve}}$ are used in this study (see Results for explanation).

Driven by the evaporation–precipitation balance, a linear relationship can be established between salinity (*S*) and the $\delta^{18}\text{O}$ of seawater ($\delta^{18}\text{O}_{\text{w}}$) (Craig and Gordon, 1965). Based on in situ measurements during the NIOP expeditions in the Red Sea, Gulf of Aden and in the western Arabian Sea, the following relationship is found for surface waters in the northwestern Arabian Sea (Delaygue et al., 2001):

$$\delta^{18}\text{O}_{\text{w, V-SMOW}} = -8.98 + 0.26S \quad (r^2 = 0.85) \quad (3)$$

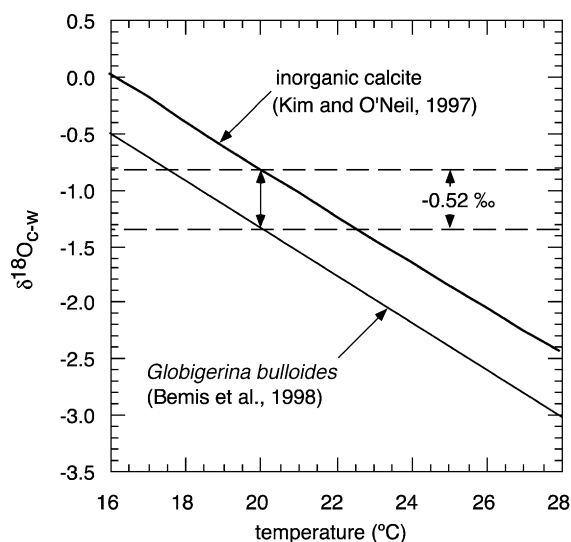


Fig. 3. Relationship between temperature and $\delta^{18}\text{O}_{\text{c-w}}$ of inorganic calcite (Kim and O’Neil, 1997). In order to calculate the calcification temperature of *G. bulloides*, the equation of Kim and O’Neil (1997) should be corrected for a vital effect ($\delta^{18}\text{O}_{\text{ve}}$). According to Bemis et al. (1998), $\delta^{18}\text{O}_{\text{ve}}$ for *G. bulloides* is approximately -0.52‰ . The slope of both equations, for temperatures between 16 and 28 °C, is virtually identical (i.e. $-0.21 \text{‰ } ^\circ\text{C}^{-1}$).

For the purpose of temperature calculations, a correction from the V-SMOW to the V-PDB standard was applied using the equation of Hut (1987):

$$\delta^{18}\text{O}_{\text{w, V-PDB}} = 0.99973\delta^{18}\text{O}_{\text{w, V-SMOW}} - 0.27. \quad (4)$$

2.5. Carbon isotopes

Compared to the oxygen isotope composition of foraminifer shells, the processes controlling the carbon isotope composition are less understood. This is because the carbon incorporated in the shell may be derived from different sources, which are related to different processes. Nevertheless, an important challenge to study the carbon isotope composition of foraminiferal shells, is that it is related to one of the key parameters in paleoceanographic studies, viz. the $\delta^{13}\text{C}$ of the total dissolved inorganic carbon ($\delta^{13}\text{C}_{\text{DIC}}$) (Williams et al., 1977, 1981; Kahn and Williams, 1981; Bouvier-Soumagnac and Duplessy, 1985; Kroon and Ganssen, 1989; Spero, 1992; Mulitza et al., 1999). Hence, the isotopic composition of the shells may be used to reconstruct this parameter

providing information on different water masses, biological productivity and nutrient cycling in surface waters (e.g. Broecker and Peng, 1982).

The $\delta^{13}\text{C}_{\text{DIC}}$ decreases with depth in the water column (Broecker and Peng, 1982; Kroopnick, 1985), so that the $\delta^{13}\text{C}$ of planktic foraminifera should reflect depth habitat as well as the $\delta^{13}\text{C}_{\text{DIC}}$. This only is true if the foraminifera precipitate their calcite in equilibrium with the ambient water. Many studies, however, have shown that the carbon isotope composition of foraminifer shells often deviates from the ambient $\delta^{13}\text{C}_{\text{DIC}}$ (e.g. Williams et al., 1977; Shackleton and Vincent, 1978; Kahn 1979; Kahn and Williams, 1981; Oppo and Fairbanks, 1989; Kroon and Ganssen, 1989; Spero, 1992; Mulitza et al., 1999). These offsets have been attributed to so called “vital effects”, a collective noun for a suite of biologically, physically and chemically controlled processes that cause an offset between the $\delta^{13}\text{C}$ of the foraminifer shell and $\delta^{13}\text{C}_{\text{DIC}}$. Most important are (1) ontogenetic and metabolic effects (Spero and Lea, 1996), (2) temperature (Bemis et al., 2000), (3) the effects of photosynthetic utilization by symbionts (e.g. Spero and DeNiro, 1987; Spero and Williams, 1988) and (4) carbonate system effects (Spero et al., 1997; Bijma et al., 1999). Below we shortly review the impact of each of these effects on the carbon isotope composition of planktic foraminifera.

2.6. Ontogenetic/metabolic effects

As a result of ontogenetic/metabolic effects, the carbon isotope composition increases with increasing shell size (Berger et al., 1978; Kroon and Darling, 1995; Spero and Lea, 1996; Bemis et al., 2000). The $\delta^{13}\text{C}_{\text{shell}}$ size trend observed in many species of planktic foraminifera most likely results from the incorporation of ^{13}C depleted metabolic CO_2 during shell growth (e.g. Spero and Lea, 1996). The fraction of metabolic CO_2 that is incorporated in the shell decreases during shell growth: chambers grown during the juvenile-neanic phase of ontogeny are therefore depleted in ^{13}C compared to chambers grown in the adult/final stage (Bemis et al., 2000). To quantify the size trends in the stable isotope composition of the shells in our field data, we have measured shells from two sieve size fractions, i.e. 150–250 and 250–355 μm .

2.7. Temperature

Laboratory experiments suggest that temperature may also affect the $\delta^{13}\text{C}_{\text{shell}}$ (Bemis et al., 2000). These authors have shown that the $\delta^{13}\text{C}_{\text{shell}}$ of *G. bulloides* follows a slope of $-0.11\text{‰ }^{\circ}\text{C}^{-1}$. Apparently, the fraction of metabolic CO_2 that is incorporated in the shell increases with temperature as a result of higher metabolic rates at higher temperatures. In field studies, however, this temperature effect is difficult to separate from other factors, such as for example carbonate system effects (Russell and Spero, 2000), since the carbonate system parameters and the temperature of seawater are often highly correlated. For species that have not been studied in culture experiments and for which the temperature effect is thus not known, a multiple regression may be used to estimate the relative contribution of carbonate system effects and temperature on the $\delta^{13}\text{C}_{\text{shell}}$ (see for example Ithou et al., 2001 for *Globorotalia scitula*).

2.8. The effect of symbionts

Some planktic foraminifer species possess symbiotic algae that may, indirectly, affect the $\delta^{13}\text{C}$ of foraminiferal shells (e.g. Spero and DeNiro, 1987). The photosynthetic algae may modulate the ambient $\delta^{13}\text{C}_{\text{DIC}}$ pool of planktic foraminifera by preferential uptake of ^{12}C . The effect of symbionts on foraminiferal $\delta^{13}\text{C}$ is difficult to quantify and depends on the photosynthetic active radiation (PAR) levels, number of symbionts and symbiont activity. The contribution of each of these effects may change during the life cycle of a planktic foraminifer (e.g. Hemleben and Bijma, 1994).

2.9. Carbonate system effects

Laboratory culture experiments (Spero et al., 1997; Bijma et al., 1998, 1999) have shown that carbonate system parameters ($[\text{CO}_3^{2-}]$ or pH) may affect the $\delta^{18}\text{O}_{\text{shell}}$ and $\delta^{13}\text{C}_{\text{shell}}$. Their results indicate that an increase in the carbonate ion concentration (or pH) results in a decrease in the oxygen and carbon isotope values in the shells of different species. Spero et al. (1997) and Bijma et al. (1998) report the following slopes: $\delta^{13}\text{C}/[\text{CO}_3^{2-}] = -0.0089\text{‰ }(\mu\text{mol kg}^{-1})^{-1}$

(*G. ruber*) and $-0.012\text{‰}(\mu\text{mol kg}^{-1})^{-1}$ (*G. bulloides*) and for $\delta^{18}\text{O}/[\text{CO}_3^{2-}] = -0.0022\text{‰}(\mu\text{mol kg}^{-1})^{-1}$ (*G. ruber*) and $-0.004\text{‰}(\mu\text{mol kg}^{-1})^{-1}$ (*G. bulloides*).

In this study, we use detailed carbonate system data from the World Ocean Circulation Experiment (WOCE) (<http://whpo.ucsd.edu/data/onetime/indian/i01/i01w/index.htm>) to calculate a $[\text{CO}_3^{2-}]$ profile for each hydrographic station. We made a selection from the WOCE-IO1W data set, including only data from the upper 200 m of the water column between 50°E and 59°E and between 13°N and 20°N (transect from the Gulf of Aden parallel to the coastlines of Yemen and Oman). The carbonate ion concentrations were calculated from TCO_2 and Total Alkalinity (TA), using the software program CO2SYS (version 1.05) of Lewis and Wallace (1998). We used the constants of Weiss (1974) for K_0 (the solubility of CO_2 in seawater), Roy et al. (1993) for K_1 ($2s=2\%$) and K_2 ($2s=1.5\%$), the equilibrium constants that define the speciation of CO_2 in seawater, and Dickson (1990) for K_B (dissociation constant of borate). The effects of pressure on K_1 and K_2 are from Millero (1995) and on K_B from Millero (1979).

2.10. The $\delta^{13}\text{C}_{\text{DIC}}$

During the C1 (August 1992) and C2 (February 1993) expeditions of the RV *Tyrol*, water samples for the analysis of $\delta^{13}\text{C}_{\text{DIC}}$ were taken at discrete depths on the same stations sampled for planktic foraminifera (Moos, 2000). To estimate the $\delta^{13}\text{C}_{\text{DIC}}$ at any depth in the water column, i.e. to establish a continuous $\delta^{13}\text{C}_{\text{DIC}}$ profile at each station, we use four second order polynomial regressions of $\delta^{13}\text{C}_{\text{DIC}}$ as a function of nitrate, silicate, phosphate and potential temperature (Fig. 4). We only included data from the upper 200 m of the water column. The $\delta^{13}\text{C}_{\text{DIC}}$ values used in this study are the average values calculated using these four equations. The following regressions were established:

For phosphate (Fig. 4a):

$$\delta^{13}\text{C}_{\text{DIC}}([\text{PO}_4]) = 1.670 - 1.102[\text{PO}_4] + 1.514 \times 10^{-1}[\text{PO}_4]^2, \quad r^2 = 0.97 \quad (5)$$

For silicate (Fig. 4b):

$$\delta^{13}\text{C}_{\text{DIC}}([\text{SiO}_4]) = 1.578 - 1.536 \times 10^{-1}[\text{SiO}_4] + 3.596 \times 10^{-3}[\text{SiO}_4]^2, \quad r^2 = 0.95 \quad (6)$$

For nitrate (Fig. 4c):

$$\delta^{13}\text{C}_{\text{DIC}}([\text{NO}_3]) = 1.326 - 7.364 \times 10^{-2}[\text{NO}_3] + 8.131 \times 10^{-4}[\text{NO}_3]^2, \quad r^2 = 0.97 \quad (7)$$

For potential temperature (Fig. 4d):

$$\delta^{13}\text{C}_{\text{DIC}}(T_{\text{POT}}) = 5.256 - 6.231 \times 10^{-1}(T_{\text{POT}}) + 1.823 \times 10^{-2}(T_{\text{POT}})^2, \quad r^2 = 0.96. \quad (8)$$

2.11. Strategy

The main aim of this study is to understand how the stable isotope composition in shells of living planktic foraminifera is controlled by the seasonal changes in sea surface water hydrography and chemistry of the two monsoon seasons. Most important are the effects of temperature, $\delta^{18}\text{O}_w$, $\delta^{13}\text{C}_{\text{DIC}}$ and the effect of the carbonate ion (CIE) (Spero et al., 1997). Because most of the parameters such as T , $\delta^{18}\text{O}_w$, $\delta^{13}\text{C}_{\text{DIC}}$ and $[\text{CO}_3^{2-}]$ change with time and depth in the water column, it is essential to know when and where foraminifera build their shells. We therefore will use the oxygen isotope composition of the shells to estimate the calcification temperature and depth of the foraminifer shells in a given plankton tow sample. Our approach includes five steps. (1) For each hydrographic station, the expected oxygen isotope equilibrium profiles for different species in different size fractions are calculated. (2) The calcification temperatures for the specimens within each depth interval (plankton tow) are calculated. (3) The $\delta^{13}\text{C}_{\text{shell}}$ is corrected for the ambient $\delta^{13}\text{C}_{\text{DIC}}$ (we thus use the $\delta^{13}\text{C}_{\text{DIC}}$ that is found at the calcification depth that was calculated from the $\delta^{18}\text{O}_{\text{shell}}$). The following notation is used: $\Delta\delta^{13}\text{C}_{\text{shell-DIC}} = \delta^{13}\text{C}_{\text{shell}} - \delta^{13}\text{C}_{\text{DIC}}$. (4) The $\Delta\delta^{13}\text{C}_{\text{shell-DIC}}$ is plotted versus $[\text{CO}_3^{2-}]$ to access the effects of the carbonate ion concentration on the

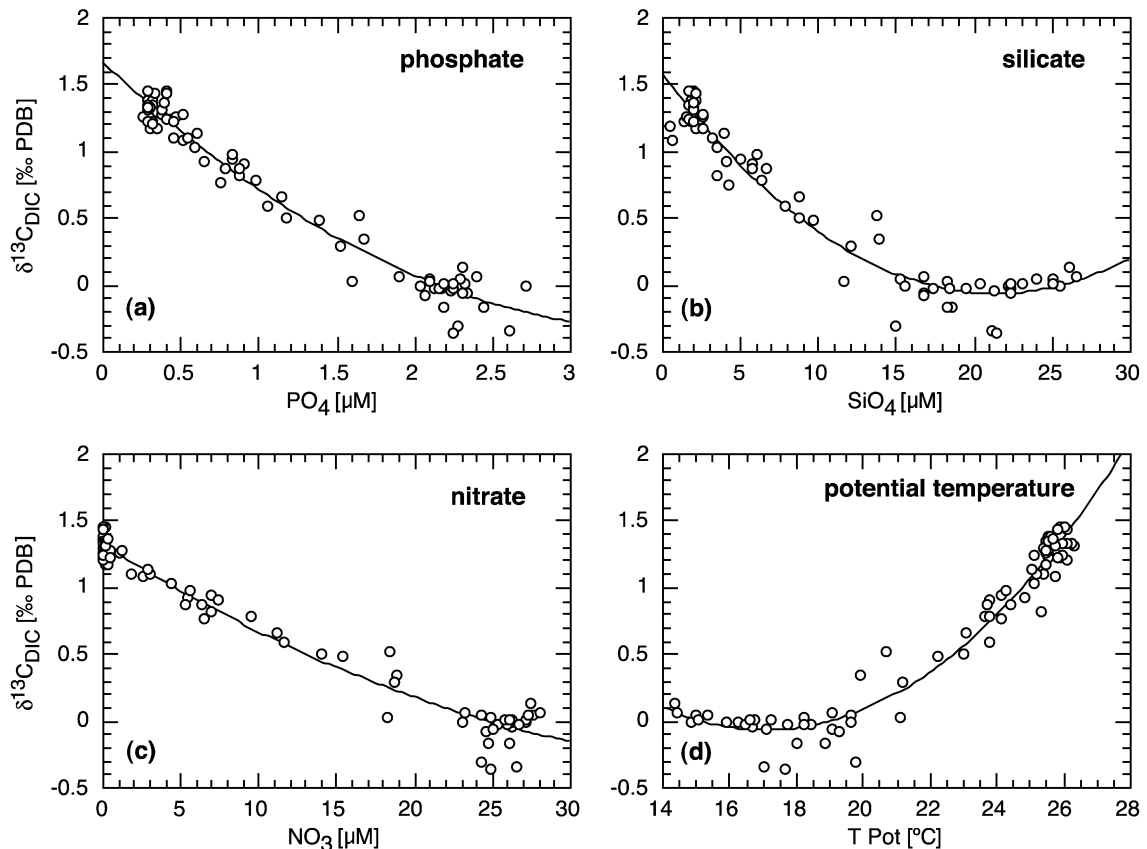


Fig. 4. Second-order polynomial fits of $\delta^{13}\text{C}$ of total dissolved inorganic carbon (DIC) as a function of (a) phosphate, (b) silicate, (c) nitrate and (d) potential temperatures. These equations are used to construct a continuous $\delta^{13}\text{C}_{\text{DIC}}$ profile at each hydrographic station.

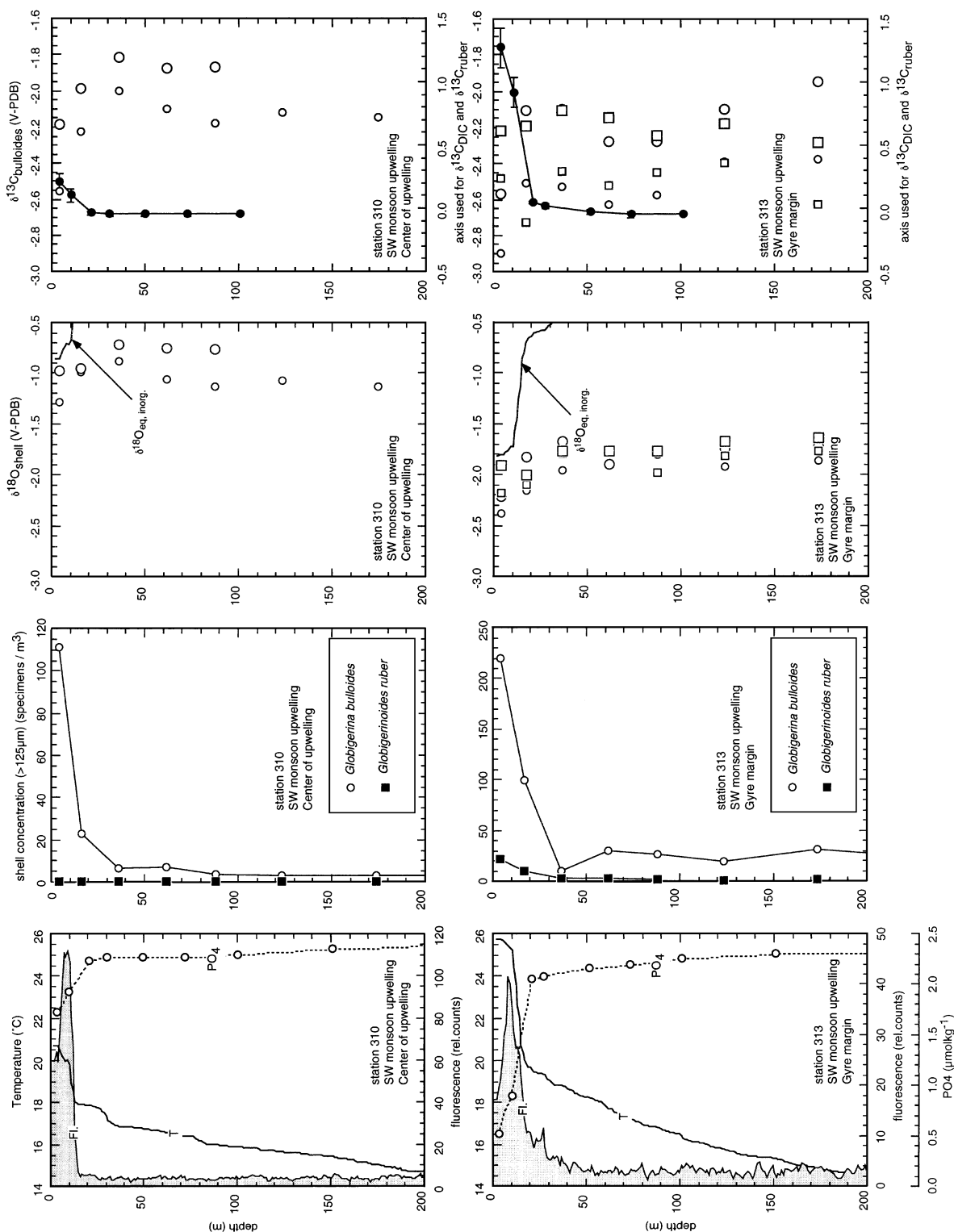
carbon isotope composition of the shells. (5) In the final step, we compare laboratory results to our field observations and discuss the implications.

3. Results

3.1. Shell concentrations

Shell concentrations (specimens m^{-3}) of *G. bulloides* ($>125 \mu\text{m}$) in the water column were two orders of magnitude higher during upwelling in August 1992 than during the non-upwelling period in March 1993 (Figs. 5 and 6, Table 2). The shell concentration decreased with depth in the water column and remained relatively constant below a depth of 25–50 m during upwelling and below 50–75 m during

non-upwelling. The low shell concentrations in the deeper plankton tows, mirror the pelagic rain of foraminiferal shells that are sinking through the water column to the seafloor. On the other hand, the higher concentrations in the upper part of the water column represent living specimens that were capable of adjusting their buoyancy to counter gravitational settling. In general, high concentrations of *G. bulloides* mirrored upwelling conditions such as found for example found in the surface waters at stations 308, 310 and 313. The latter station is of particular interest because it represented the highly productive frontal zone between the freshly upwelled waters (i.e. found at station 310) and the more oligotrophic open oceanic waters. It is thus evident from our data that high shell concentrations of *G. bulloides* were associated with upwelled waters during the SW monsoon season



whereas low concentrations were found during the NE monsoon (Figs. 5 and 6). Shell concentrations of *G. ruber*, however, were high during non-upwelling (stations 917 and 920) and lower during upwelling periods (Figs. 5 and 6, Table 2). Shells of *G. ruber* were absent in the center of coastal upwelling (stations 308 and 310), suggesting that *G. ruber* does not proliferate in the pristine upwelled water. The surface waters at station 313 also contained a high concentration of *G. ruber* shells, indicating that this species is productive during both monsoon seasons. Similar to *G. bulloides*, the shell concentration of *G. ruber* decreased with depth in the water column and remained constant below approximately 25–50 m during upwelling and below 75–100 m during non-upwelling.

3.2. Size trends in $\delta^{18}\text{O}_{\text{shell}}$ and quantification of the vital effect

For both *G. bulloides* and *G. ruber*, the oxygen isotope composition of larger specimens (in the 250–355 μm size fraction) is higher than those in the 150–250 μm size fraction (Fig. 7, Table 2). In the center of upwelling, station 310, large shells of *G. bulloides* are on average $0.27 \pm 0.13\text{‰}$ higher compared to smaller ones. In the surface sample (SST=20.3 °C), where both large and small specimens calcify under equal environmental conditions, this difference is 0.31‰ (Table 2). At station 313, large shells of *G. bulloides* are on average $0.21 \pm 0.11\text{‰}$ higher compared to smaller ones. In the surface sample (SST=25.5 °C), this difference is 0.17‰ (Figs. 7 and 8, Table 2). Apparently, the oxygen isotope difference between large and small shells, the ontogenetic effect, is not constant and decreases with temperature (Fig. 8). This observation confirms the results of Bemis et al. (1998) who reported: “...Successive chambers are progressively enriched in ^{18}O relative to earlier ones, although the $\delta^{18}\text{O}$ values appear to converge at higher temperatures...”. To quantify the temperature-dependent ontogenetic effect of *G. bulloides*, we use the data

from the shallowest plankton net at station 310 (i.e. 0.31‰ at 20.3 °C) and station 313 (i.e. 0.17‰ at 25.5 °C) to establish the following relationship:

$$\Delta\delta^{18}\text{O}_{\text{large-small}} = 0.84 - 0.026T \quad (9)$$

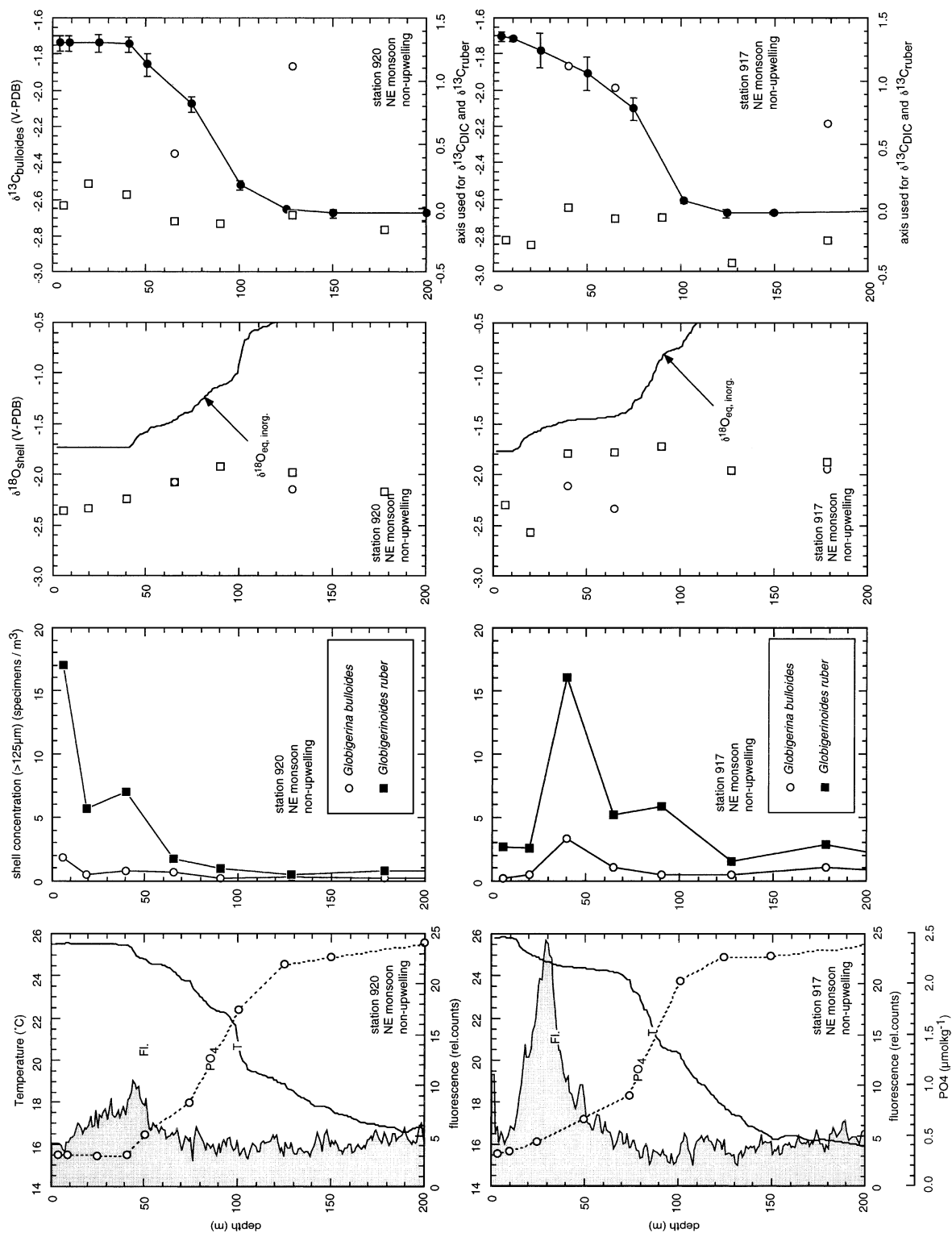
in which $\Delta\delta^{18}\text{O}_{\text{large-small}}$ represents the difference between the $\delta^{18}\text{O}_{\text{shell}}$ of specimens in the 250–355 and 150–250 μm size fractions.

In addition, the oxygen isotope composition of the specimens may be affected by the carbonate ion concentration of the ambient seawater. In literature, however, only $\delta^{18}\text{O}_{\text{c-w}}/[\text{CO}_3^{2-}]$ relationships for individual chambers in the shell whorl are reported (Spero et al., 1997). Unfortunately, no data or estimates are available on the effect of the carbonate ion concentration for whole shells. We therefore must calculate the magnitude of this effect from our field data. At stations 310 and 313, the expected $\delta^{18}\text{O}_{\text{eq}}$ for inorganic calcite, using the equation of Kim and O’Neil (1997), is -0.89‰ and -1.96‰ , respectively. The carbonate ion concentration in surface waters of stations 310 and 313 is 140 ± 12 and $243 \pm 13 \mu\text{mol kg}^{-1}$, respectively. Consequently, the difference between the observed $\delta^{18}\text{O}_{\text{shell}}$ values and the expected $\delta^{18}\text{O}_{\text{eq}}$ for inorganic calcite may be attributed to carbonate system effects. For *G. bulloides* in the 250–355 μm size fraction, we find the following relationship:

$$\delta^{18}\text{O}_{\text{large}} - \delta^{18}\text{O}_{\text{eq. inorg.}} = 0.17 - 0.0025[\text{CO}_3^{2-}] \quad (10)$$

Apparently, the slope we find for the carbonate ion effect on the oxygen isotope composition for whole shells is smaller than the -0.005 and -0.004‰ ($\mu\text{mol kg}^{-1}$) $^{-1}$ reported by Spero et al. (1997) for the 12th and 13th chamber. Consequently, we may conclude that the ontogenetic effect in shells of *G. bulloides* decreases with increasing temperature with a slope of $-0.026\text{‰ } ^\circ\text{C}^{-1}$, whereas the carbonate ion concentration in seawater decreases the $\delta^{18}\text{O}_{\text{shell}}$

Fig. 5. Graph showing hydrographic conditions (temperature, fluorescence and phosphate concentration), shell concentration profile (>125 μm) and stable isotope composition of *G. bulloides* and *G. ruber* from size fractions 150–250 and 250–355 μm , at stations 310 and 313 during upwelling conditions in August 1992.



with a slope of $-0.0025\text{‰} (\mu\text{mol kg}^{-1})^{-1}$. These results suggest that the calcification temperatures for *G. bulloides* shells can be calculated using:

$$\begin{aligned}\delta^{18}\text{O}_{\text{shell}}(150-250) &= \delta^{18}\text{O}_{\text{eq. inorg.}} - 0.67 \\ &\quad - 0.0025[\text{CO}_3^{2-}] \\ &\quad + 0.026T + \delta^{18}\text{O}_{\text{w}}\end{aligned}\quad (11)$$

$$\begin{aligned}\delta^{18}\text{O}_{\text{shell}}(250-355) &= \delta^{18}\text{O}_{\text{eq. inorg.}} + 0.17 \\ &\quad - 0.0025[\text{CO}_3^{2-}] \\ &\quad + \delta^{18}\text{O}_{\text{w}}.\end{aligned}\quad (12)$$

For shells of *G. ruber*, the ontogenetic effect between large and small shells is 0.26‰ in the surface plankton net of station 313 (at 25.5 °C). An average of all samples from this station yields $\Delta\delta^{18}\text{O}_{\text{large-small}} = 0.17 \pm 0.13\text{‰}$ (Fig. 7, Table 2). Given that no “large” *G. ruber* specimens were measured at other stations, it is not possible to determine if the ontogenetic effect is temperature dependent. Non-upwelling stations 917 and 920, however, allow a detailed calculation of the vital effect of specimens in the $150\text{--}250\text{ }\mu\text{m}$ size fraction: the difference between the observed oxygen isotope composition of the shells and expected $\delta^{18}\text{O}_{\text{eq}}$ for inorganic calcite is -0.54‰ and -0.63‰ at station 917 and 920, respectively. Consequently, we will use the maximum estimate (-0.63‰) for the $150\text{--}250\text{ }\mu\text{m}$ size fraction and a value of -0.37‰ ($= -0.63 + 0.26$) for the $250\text{--}355\text{ }\mu\text{m}$ size fraction. The carbonate ion concentration in surface waters of stations 917 and 920 is virtually constant ($250\text{--}253\text{ }\mu\text{mol kg}^{-1}$) and does not allow an estimate of the carbonate ion effect on $\delta^{18}\text{O}_{\text{rub.}}$. To calculate the expected equilibrium value for shells of *G. ruber*, we therefore will use the $\Delta\delta^{18}\text{O}_{\text{shell-w}}/[\text{CO}_3^{2-}]$ slope of Bijma et al. (1998) of $-0.0022\text{‰} (\mu\text{mol kg}^{-1})^{-1}$, relative to the ambient $[\text{CO}_3^{2-}]$ value of surface waters

at stations 917 and 920 ($\approx 250\text{ }\mu\text{mol kg}^{-1}$). This yields the following temperature equations for shells of *G. ruber*:

$$\begin{aligned}\delta^{18}\text{O}_{\text{ruber}}(150-250) &= \delta^{18}\text{O}_{\text{eq. inorg.}} - 0.63 \\ &\quad - 0.0022([\text{CO}_3^{2-}] \\ &\quad - 250) + \delta^{18}\text{O}_{\text{w}}\end{aligned}\quad (13)$$

$$\begin{aligned}\delta^{18}\text{O}_{\text{ruber}}(250-355) &= \delta^{18}\text{O}_{\text{eq. inorg.}} - 0.37 \\ &\quad - 0.0022([\text{CO}_3^{2-}] \\ &\quad - 250) + \delta^{18}\text{O}_{\text{w}}.\end{aligned}\quad (14)$$

3.3. Calcification temperatures

The calcification temperatures of *G. bulloides* suggest that this species grows in the upper 15 m during upwelling (stations 308, 310 and 313) and around 50 and 60 m during non-upwelling (stations 917 and 920), hence, reflecting temperatures at or just below the depth of the DCM (Table 2). On average, the calcification temperature of *G. bulloides* was $1.3 \pm 0.9\text{ °C}$ lower than the sea surface temperature.

The calcification temperatures of *G. ruber* mirrored the seawater temperatures near the DCM, at 11 m during upwelling (at station 313). Although calcification temperatures during non-upwelling ranged between the sea surface temperatures and those found at 80 m, the average calcification temperatures suggest that most calcite precipitated between 50 and 80 m, i.e. between the DCM and the upper thermocline. On average, the calcification temperature of *G. ruber* was $1.7 \pm 0.8\text{ °C}$ lower than the sea surface temperature.

3.4. The carbon isotope composition of *G. bulloides*

Above we used the $\delta^{18}\text{O}$ of *G. bulloides* to estimate the calcification temperature and depth. Although the specimens may migrate during their life cycle and build parts of their shells at different depths

Fig. 6. Graph showing hydrographic conditions (temperature, fluorescence and phosphate concentration), shell concentration profile ($>125\text{ }\mu\text{m}$) and stable isotope composition of *G. bulloides* and *G. ruber* from size fractions $150\text{--}250\text{ }\mu\text{m}$ and $250\text{--}355\text{ }\mu\text{m}$, at stations 920 and 917 during non-upwelling conditions in February–March 1993.

Overview of hydrographic stations in August 1992 and stable isotope composition of *G. bulloides* and *G. ruber*

Sample (Station – cast – net)	Date/Time (GMT + 3)	Depth start (m)	Depth end (m)	T_{start} (°C)	T_{end} (°C)	Salinity (per mil)	$\delta^{13}\text{C}_{\text{DIC}}$ (VPDB)	S.D. on $\delta^{13}\text{C}_{\text{DIC}}$	<i>G. bul</i> >125 μm (ind./m ³)	<i>G. rub</i> >125 μm (ind./m ³)
308–1–5	19/08/1992	23	0	17.5	20.5	35.65	0.07	0.03	91.22	0.16
308–1–4	09.25 h	48	23	16.9	17.5	35.64	0.02	0.02	11.20	0.00
308–1–3		72	48	16.4	16.9	35.63	0.01	0.02	8.28	0.03
308–1–2		98	72	15.8	16.4	35.64	0.01	0.01	2.81	0.20
Average S.D.										
310–5–5	20/08/1992	8	0	20.0	20.7	35.66	0.20	0.08	111.09	0.00
310–5–4	15.37 h	23	8	17.8	20.0	35.66	0.05	0.02	22.83	0.00
310–5–3		49	23	16.8	17.8	35.64	0.02	0.02	6.00	0.00
310–5–2		74	49	16.4	16.8	35.64	0.01	0.02	6.60	0.07
310–5–1		100	74	15.9	16.4	35.63	0.01	0.01	3.56	0.04
310–6–4	20/08/1992	148	98	15.4	15.9	35.67	0.03	0.03	2.90	0.04
310–6–3	17.08 h	200	148	14.6	15.4	35.68	0.05	0.04	2.67	0.05
310–6–2		298	200	13.6	14.6	35.68			2.67	0.04
310–6–1		498	298	12.0	13.6	35.71			2.79	0.05
Average S.D.										
313–4–5	21/08/1992	8	0	25.3	25.7	35.97	1.24	0.25	219.04	20.96
313–4–4	12.10 h	24	10	19.4	25.3	35.73	0.29	0.06	98.57	9.27
313–4–3		49	24	18.3	19.4	35.67	0.08	0.02	9.81	2.01
313–4–2		74	50	17.2	18.3	35.64	0.03	0.02	29.07	2.47
313–4–1		100	75	16.5	17.2	35.63	0.01	0.02	26.07	1.24
313–dc–4	22/08/1992	148	99	15.4	16.5	35.62	0.01	0.02	18.75	0.57
313–dc–3	13.49 h	196	150	14.5	15.4	35.66	0.05	0.03	30.98	0.69
313–dc–2		300	199	13.4	14.5	35.70			18.22	0.54
313–dc–1		498	300	11.8	13.4	35.71			32.78	0.73
Average S.D.										
917–2–5	25/02/1993	12	0	25.7	25.8	36.20	1.36	0.07	0.19	2.60
917–2–4	09.15 h	27	12	24.9	25.7	36.23	1.23	0.18	0.48	2.55
917–2–3		52	27	24.3	24.9	36.26	1.10	0.29	3.35	16.01
917–2–2		78	52	23.1	24.3	36.24	0.99	0.31	1.08	5.22
917–2–1		102	78	20.0	23.1	35.91	0.37	0.10	0.45	5.84
917–1–4	26/02/1993	153	101	16.3	20.0	35.73	0.05	0.07	0.52	1.53
917–1–3	08.30 h	203	153	15.7	16.3	35.80	0.07	0.13	1.09	2.82
917–1–2		302	203	13.8	15.7	35.82			0.14	0.72
917–1–1		502	302	11.9	13.8	35.71			0.39	1.42
Average S.D.										
920–2–5	27/02/1993	11	0	25.5	25.5	36.12	1.27	0.07	1.83	17.00
920–2–4	0.915 h	27	11	25.5	25.5	36.12	1.26	0.07	0.44	5.71
920–2–3		53	27	24.6	25.5	36.12	1.20	0.07	0.74	7.00
920–2–2		78	53	23.1	24.6	36.15	0.97	0.18	0.65	1.75
920–2–1		102	78	19.9	23.1	35.98	0.54	0.12	0.18	0.99
920–1–4	27/02/1993	153	103	17.5	19.9	35.78	0.10	0.10	0.25	0.52
920–1–3	0.815 h	202	153	16.5	17.5	35.75	0.05	0.09	0.16	0.74
920–1–2		303	202	14.0	16.5	35.90			0.18	0.69
920–1–1		501	303	12.6	14.0	35.75			0.26	1.18
Average S.D.										

$\delta^{13}\text{C}_{\text{bul}}$ (150–250)	$\delta^{18}\text{O}_{\text{bul}}$ (150–250)	$\delta^{13}\text{C}_{\text{bul}}$ (250–355)	$\delta^{18}\text{O}_{\text{bul}}$ (250–355)	$\delta^{13}\text{C}_{\text{rub}}$ (150–250)	$\delta^{18}\text{O}_{\text{rub}}$ (150–250)	$\delta^{13}\text{C}_{\text{rub}}$ (250–355)	$\delta^{18}\text{O}_{\text{rub}}$ (250–355)	T _{bul} (150–250)	T _{bul} (250–355)	T _{rub} (150–250)	T _{rub} (250–355)
		– 2.07	– 1.02							20.26	
		– 1.91	– 1.10							20.52	
		– 1.96	– 1.04							20.34	
		– 1.98	– 1.05							20.37	
		0.08	0.04							0.13	
– 2.56	– 1.29	– 2.19	– 0.98					20.41		20.38	
– 2.23	– 0.99	– 1.99	– 0.96					19.09		20.31	
– 2.00	– 0.89	– 1.82	– 0.72					18.60		19.34	
– 2.10	– 1.06	– 1.88	– 0.76					19.40		19.52	
– 2.18	– 1.14	– 1.87	– 0.77					19.77		19.55	
– 2.12	– 1.08							19.50			
– 2.15	– 1.14							19.76			
– 2.36	– 1.47	– 1.73	– 1.03					21.13		20.61	
– 1.82	– 1.14	– 1.81	– 0.90					19.76		20.08	
– 2.17	– 1.13	– 1.90	– 0.87					19.71		19.97	
0.21	0.17	0.15	0.12					0.73		0.50	
– 2.90	– 2.39	– 2.57	– 2.22	0.24	– 2.18	0.61	– 1.91	25.56	25.56	24.69	24.67
– 2.51	– 2.16	– 2.11	– 1.83	– 0.11	– 2.10	0.65	– 2.01	24.50	24.01	24.38	25.06
– 2.53	– 1.96	– 2.10	– 1.68	0.29	– 1.80	0.77	– 1.77	23.62	23.39	23.17	24.11
– 2.63	– 1.89	– 2.28	– 1.90	0.18	– 1.76	0.72	– 1.77	23.32	24.26	22.99	24.12
– 2.58	– 1.99	– 2.28	– 1.80	0.28	– 1.99	0.58	– 1.77	23.75	23.86	23.92	24.11
– 2.39	– 1.93	– 2.10	– 1.75	0.36	– 1.82	0.67	– 1.68	23.51	23.67	23.24	23.73
– 2.38	– 1.87	– 1.95	– 1.72	0.03	– 1.77	0.52	– 1.64	23.23	23.55	23.03	23.56
– 2.36	– 1.93	– 1.84	– 1.72	0.31	– 1.85	0.43	– 1.55	23.51	23.55	23.38	23.19
– 2.19	– 1.93	– 2.00	– 1.57	0.34	– 1.79	0.52	– 1.43	23.48	22.96	23.10	22.68
– 2.50	– 2.01	– 2.14	– 1.80	0.21	– 1.90	0.61	– 1.73	23.83	23.87	23.54	23.91
0.20	0.17	0.22	0.18	0.16	0.15	0.11	0.18	0.74	0.73	0.63	0.73
				– 0.25	– 2.30					25.40	
– 1.87	– 2.11			0.00	– 1.80			24.54		23.35	
– 1.99	– 2.34			– 0.08	– 1.78			25.51		23.25	
				– 0.07	– 1.73					23.05	
				– 0.43	– 1.96					24.04	
– 2.19	– 1.95			– 0.25	– 1.88			23.85		23.71	
				– 0.34	– 1.91					23.80	
– 1.86	– 1.83			– 0.26	– 1.88			23.29		23.69	
– 1.98	– 2.06			– 0.21	– 1.90			24.30		23.79	
0.15	0.22			0.15	0.18			0.96		0.73	
				0.02	– 2.36					25.50	
				0.19	– 2.34					25.45	
				0.10	– 2.24					25.08	
– 2.35	– 2.08			– 0.10	– 2.08			24.32		24.46	
				– 0.12	– 1.93					23.85	
– 1.87	– 2.15			– 0.06	– 1.98			24.61		24.02	
				– 0.17	– 2.17					24.80	
– 2.10	– 2.11			– 0.11	– 2.10			24.47		24.50	
				– 0.62	– 2.19					24.87	
– 2.11	– 2.11			– 0.10	– 2.16			24.47		24.72	
0.24	0.03			0.23	0.15			0.15		0.58	

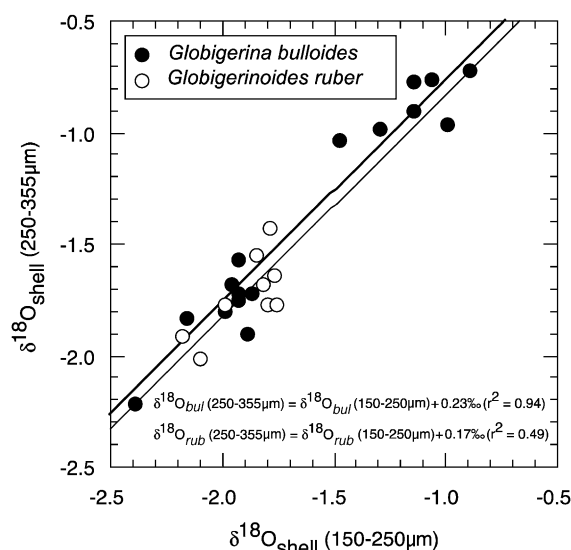


Fig. 7. The oxygen isotope composition of *G. bulloides* and *G. ruber* from two size fractions. On average, large shells are enriched in ^{18}O compared to smaller ones by 0.23‰ (*G. bulloides*) and 0.17‰ (*G. ruber*).

in the water column, the “final” $\delta^{18}\text{O}$ of the shells will record a intermediate calcification depth biased towards the depth at which most calcite has been precipitated, i.e. the last few chambers. For reasons of simplicity, we therefore assume in this study that a given specimen precipitates its whole shell at a single depth level in the water column. Consequently, we used the ambient $\delta^{13}\text{C}_{\text{DIC}}$ of this depth to correct the $\delta^{13}\text{C}_{\text{shell}}$.

The $\delta^{13}\text{C}$ of *G. bulloides* ranges between -2.90‰ and -1.81‰ (Table 2). No relation between the oxygen and carbon isotope composition is found if all measured (“raw”), data are plotted (Fig. 9a). The $\delta^{13}\text{C}$ values of *G. bulloides* are higher in the pristine upwelled waters (stations 308 and 310) compared to $\delta^{13}\text{C}$ values at station 313 (upwelling eddy). Surprisingly, $\delta^{13}\text{C}$ values of *G. bulloides* during non-upwelling are close to the upwelling values of stations 308 and 310. The carbon isotope composition of *G. bulloides* appears to be size dependent. In the centre of upwelling, station 310, the $\delta^{13}\text{C}$ of *G. bulloides* in the size fraction $150\text{--}250\text{ }\mu\text{m}$ average at $-2.17 \pm 0.21\text{‰}$, whereas the values in the fraction $250\text{--}355\text{ }\mu\text{m}$ are consistently higher and average at $-1.90 \pm 0.15\text{‰}$ (Table 2). At station 313, the $\delta^{13}\text{C}_{\text{bul}}$ average at

$-2.50 \pm 0.20\text{‰}$ and $-2.14 \pm 0.22\text{‰}$ in the smaller and larger fraction, respectively. At non-upwelling stations 920 and 917, only the $150\text{--}250\text{ }\mu\text{m}$ fraction was measured. We find an average of $-2.11 \pm 0.24\text{‰}$ and $-1.98 \pm 0.15\text{‰}$ at stations 920 and 917, respectively (Table 2). If we correct the $\delta^{13}\text{C}_{\text{bul}}$ data for the ambient $\delta^{13}\text{C}_{\text{DIC}}$ at the calcification depth, positive linear relationships between $\Delta\delta^{18}\text{O}_{\text{bul-w}}$ and $\Delta\delta^{13}\text{C}_{\text{bul-DIC}}$ are found for the different size fractions (Fig. 9b). The two regressions converge at higher temperatures (lower $\delta^{18}\text{O}_{\text{shell-w}}$ values), confirming the temperature-dependent ontogenetic effect between the two size fractions, which decreases with temperature (Bemis et al., 2000).

A closer look at the carbon isotope variability in shells of *G. bulloides* shows that the $\Delta\delta^{13}\text{C}_{\text{bul-DIC}}$ values correlate well with (the calcification) temperature (Fig. 10a). We find slopes of -0.22‰ and $-0.23\text{‰ } ^\circ\text{C}^{-1}$ for the small and large fraction, respectively. This is about two times the gradient reported from culture experiments (Bemis et al., 2000). These authors suggest a temperature effect on the carbon isotope composition of *G. bulloides* of $-0.11\text{‰ } ^\circ\text{C}$. However, since temperature and the carbonate ion concentration in seawater are correlated with one another (Fig. 2), the changes in the $\Delta\delta^{13}\text{C}_{\text{bul-DIC}}$ also correlate well with the carbonate ion concentration. Consequently, a scatter plot of the

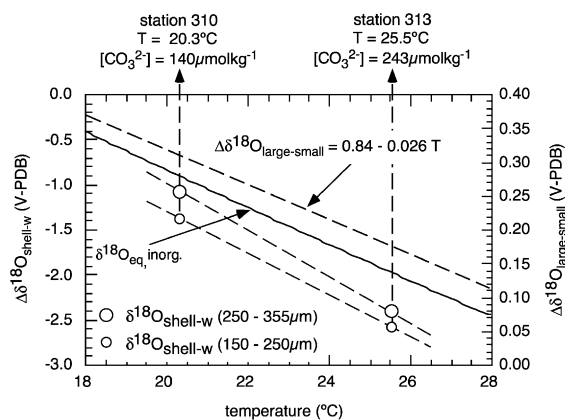


Fig. 8. The ontogenetic effect in shells of *G. bulloides* is temperature dependent. The difference between large and small shells at stations 310 and 313 decreases with temperature. The offset from the $\delta^{18}\text{O}_{\text{eq, inorg.}}$ (Kim and O’Neil, 1997) is attributed to the carbonate ion effect. See text for discussion.

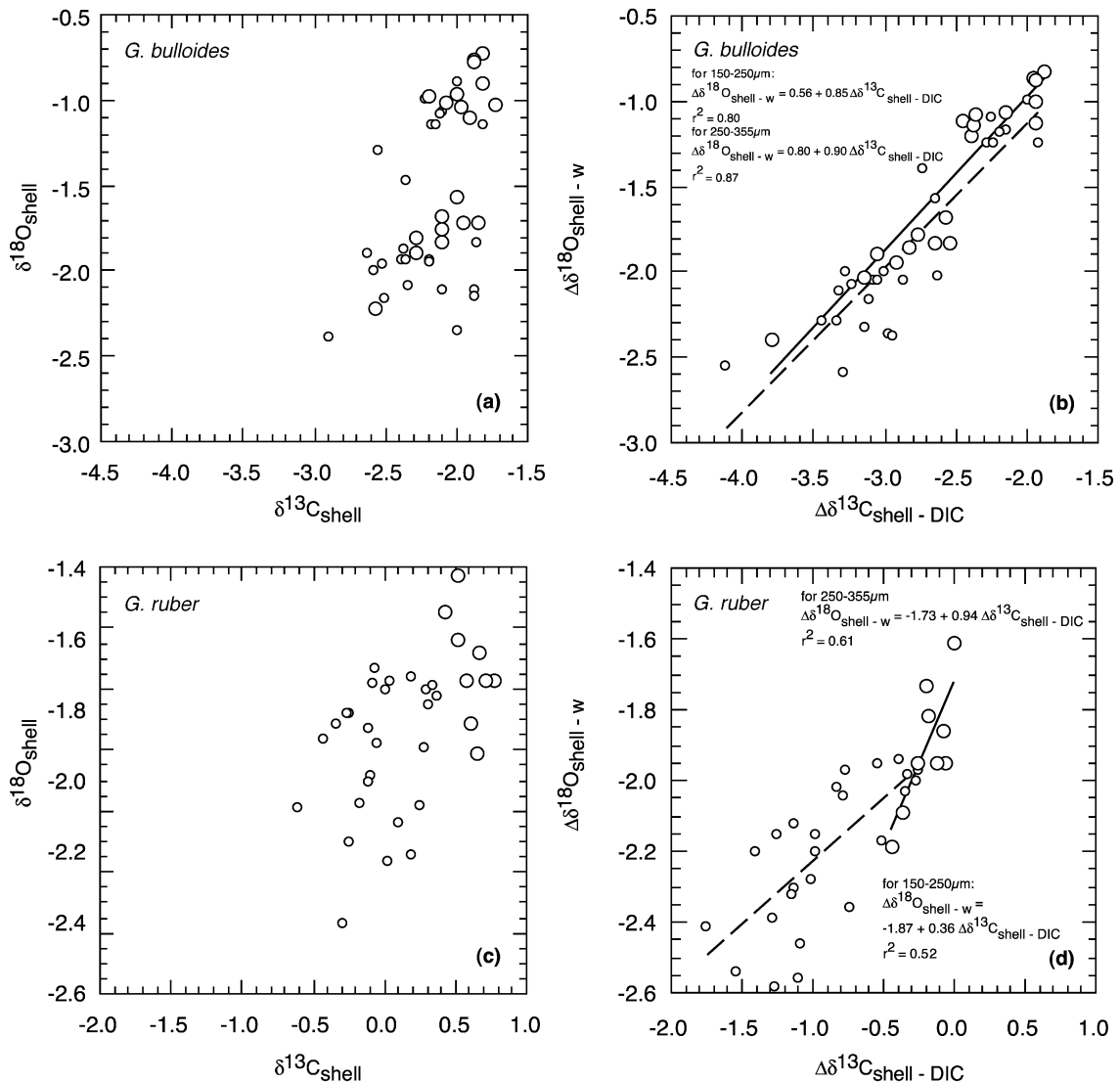


Fig. 9. (a) Scatter plot of measured (“raw”) $\delta^{13}\text{C}_{\text{shell}}$ and $\delta^{18}\text{O}_{\text{shell}}$ data for *G. bulloides*. (b) Scatter plot of $\delta^{18}\text{O}_w$ and $\delta^{13}\text{C}_{\text{DIC}}$ corrected shell values. The lines indicate linear regressions for the different size fractions: dashed line for 150–250 μm , solid line for 250–355 μm . (c–d) Same as plots (a–b), but now for *G. ruber*. Small circles indicate measurements on specimens from the 150–250 μm size fraction, large circles refer to measurements from the 250–355 μm size fraction.

$\Delta\delta^{13}\text{C}_{\text{bul-DIC}}$ versus the carbonate ion concentration, yields slopes of -0.012‰ and -0.013‰ ($\mu\text{mol kg}^{-1}$) $^{-1}$ for specimens in the 150–250 and 250–355 μm fractions, respectively (Fig. 10d). Remarkably, these slopes are identical to those reported by Spero et al. (1997) for the 12th and 13th chamber of specimens of *G. bulloides* that were grown under

controlled conditions in laboratory culture experiments.

3.5. The carbon isotope composition of *G. ruber*

The $\delta^{13}\text{C}$ of the symbiotic species *G. ruber* ranges between -0.62‰ and $+0.77\text{‰}$ (Table 2). If shell

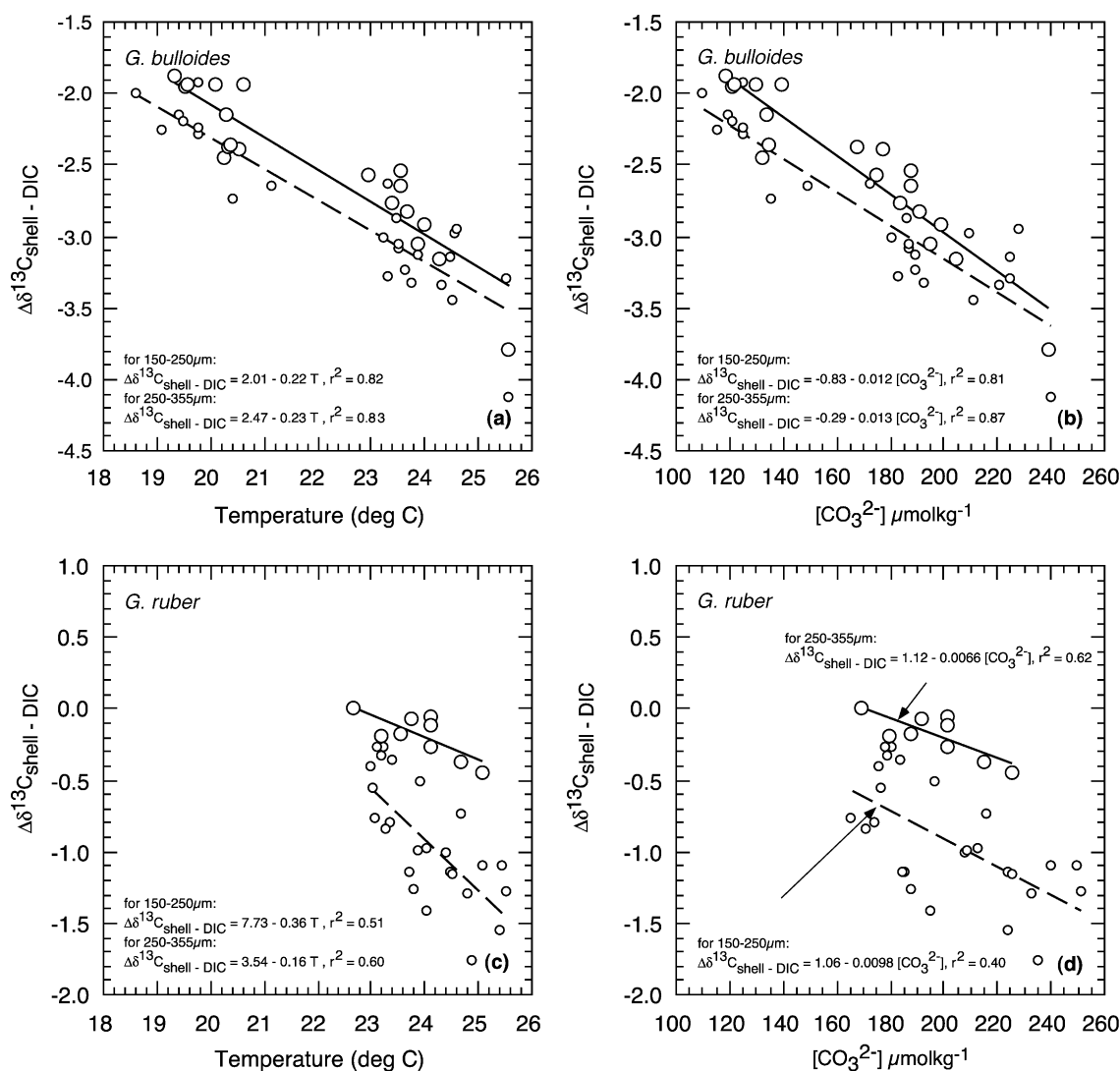


Fig. 10. Scatter plot of the $\delta^{13}\text{C}_{\text{DIC}}$ corrected $\delta^{13}\text{C}_{\text{shell}}$ values for *G. bulloides* ($\delta^{13}\text{C}_{\text{bul-DIC}}$) versus (a) temperature and (b) the carbonate ion concentration. Lines indicate linear regressions: dashed line for 150–250 μm , solid line for 250–355 μm . (c–d) Same as (a–b) for *G. ruber*. Small circles indicate measurements on specimens from the 150–250 μm size fraction, large circles refer to measurements from the 250–355 μm size fraction. Due to ontogenetic effects, different relationships for “small” and “large” specimens are found. See text for discussion.

values are not corrected for $\delta^{18}\text{O}_w$ and $\delta^{13}\text{C}_{\text{DIC}}$, the $\delta^{18}\text{O}_{\text{rub}}$ and $\delta^{13}\text{C}_{\text{rub}}$ appear uncorrelated (Fig. 9c). When the oxygen isotope composition of the shells is used to estimate the calcification depth and the in situ $\delta^{13}\text{C}_{\text{DIC}}$ value is subtracted from the carbon isotope composition of the shells, positive linear relationships between $\Delta\delta^{18}\text{O}_{\text{rub-w}}$ and $\Delta\delta^{13}\text{C}_{\text{rub-DIC}}$ are found (Fig. 9d). Although the number of data on specimens in the

large size fraction is rather small ($N=9$) and all originate from station 313, a steeper $\Delta\delta^{18}\text{O}_{\text{rub-w}}/\Delta\delta^{13}\text{C}_{\text{rub-DIC}}$ slope for large specimens may be recognized. Furthermore, the $\delta^{13}\text{C}_{\text{rub}}$ data from station 313 show that specimens in the 250–355 μm fraction are on average $+0.40\text{‰}$ higher in the 250–355 μm fraction ($0.61 \pm 0.11\text{‰}$) compared to the specimens in the 150–250 μm fraction ($0.21 \pm 0.16\text{‰}$) (Fig. 5, Table

2). This size-trend may be attributed to: (1) an (temperature dependent?) metabolic effect and/or (2) the effect of symbionts or symbiont activity.

In Fig. 10c, the $\Delta\delta^{13}\text{C}_{\text{rub-DIC}}$ is plotted versus temperature, suggesting a $\Delta\delta^{13}\text{C}_{\text{rub-DIC}}/T$ slope of -0.16‰ and $-0.36\text{‰ } ^\circ\text{C}^{-1}$ for the small and large fraction, respectively. However, when the $\Delta\delta^{13}\text{C}_{\text{rub-DIC}}$ values are plotted versus the carbonate ion concentration (Fig. 10d), we find $\Delta\delta^{13}\text{C}_{\text{rub-DIC}}/[\text{CO}_3^{2-}]$ slopes for small ($-0.0066\text{‰ } (\mu\text{mol kg}^{-1})^{-1}$) and large specimens ($-0.0098\text{‰ } (\mu\text{mol kg}^{-1})^{-1}$) that are virtually parallel. Similar to our results for *G. bulloides*, it appears that the $\Delta\delta^{13}\text{C}_{\text{rub-DIC}}/[\text{CO}_3^{2-}]$ slope from our field data is close to the one established from laboratory culture experiments: Bijma et al. (1998) reported a $\Delta\delta^{13}\text{C}_{\text{rub-DIC}}/[\text{CO}_3^{2-}]$ slope for *G. ruber* of $-0.0089\text{‰ } (\mu\text{mol kg}^{-1})^{-1}$.

4. Discussion

Previous studies have indicated that information on preferred depth habitat, season of growth and seawater chemistry is essential to unravel the stable isotope signatures of planktic foraminifera (i.e. Kroon and Ganssen, 1989; Curry et al., 1992; Steens et al., 1992; Niebler et al., 1999). The central objective of this study is to identify and quantify those mechanisms that control stable isotope composition in modern shells of planktic foraminifera in the upwelling area of the NW Arabian Sea. This knowledge is essential to solve some potential problems that are encountered when interpreting the stable isotope record of fossil specimens in deep-sea cores. Only if fundamentally understood, the fossil stable isotope record can be applied to reconstruct the paleoceanographic changes of surface waters.

The results from our plankton tow measurements show that the stable isotope composition in shells of *G. bulloides* and *G. ruber* is strongly controlled by the seasonal changes in surface water hydrography that are dictated by the mode of the monsoon cycle. Seasonal upwelling causes large changes in surface water conditions directly affecting the physical and chemical environment in which foraminifera precipitate their calcite shells.

In this study, we show that the oxygen isotope composition of the shells must be corrected for a

“vital effect” in order to calculate calcification temperatures accurately. Among others, we found that small specimens are depleted in ^{18}O compared to larger ones. We have shown that the “vital effect” is not a constant number, but depends on the ambient temperature and/or carbonate ion concentration. For example, the difference in the oxygen isotope composition between large (250–355 μm) and small (150–250 μm) shells of *G. bulloides* decreases with increasing temperature ($-0.026\text{‰ } ^\circ\text{C}^{-1}$). In general, the $\Delta\delta^{18}\text{O}_{\text{shell-w}}$ values reflect the temperatures in the upper water column between the DCM and the upper thermocline. This may be indicative for the importance of the DCM as a food source for planktic foraminifera and as such the major control for the depth habitat of shallow dwelling spinose species (Fairbairns and Wiebe, 1980). During the SW monsoon upwelling-season the DCM is found close to the sea surface and both species have a shallower depth habitat compared to the NE monsoon. The calcification temperatures and shell concentration profiles suggest that the depth habitat of *G. bulloides* is not much different from *G. ruber*. Consequently, the difference between the oxygen isotope composition of these two species ($\Delta\delta^{18}\text{O}_{\text{bul-rub}}$) in the fossil record must result from the seasonal differences in shell production. Because shell concentrations of *G. bulloides* are two orders of magnitude higher during upwelling than during non-upwelling, fossil specimens of this species only mirror the surface water conditions during the SW monsoon upwelling season. Sediment trap studies in the Arabian Sea confirm that high fluxes of this species are restricted to the summer SW monsoon (Curry et al., 1992; Conan and Brummer, 2000). Consequently, the observed variability in the stable isotope composition of *G. bulloides* in the fossil record must be attributed to changes in SST, productivity ($\delta^{13}\text{C}_{\text{DIC}}$) and surface water carbonate chemistry during the upwelling season. In addition, our results show that *G. ruber* produces shells during both monsoon seasons. Due to a higher optimum temperature and the fact that this species may obtain nutrition from its symbionts, it proliferates in relatively warm and oligotrophic surface waters. Because shell production of *G. bulloides* is restricted to upwelling period and *G. ruber* produces shells during both monsoon seasons, the $\Delta\delta^{18}\text{O}_{\text{bul-rub}}$ may be used as a proxy for seasonal surface water temperature

variations (e.g. Peeters, 2000). Simultaneous use of this proxy with surface water temperature estimates, derived from faunal transfer-functions or U_{37}^k ratios, may provide a useful tool to estimate past surface water temperature variations.

The $\delta^{13}C$ of the foraminiferal shells is affected by at least three to four factors: (1) The $\delta^{13}C_{DIC}$, (2) the carbonate ion concentration in seawater, (3) ontogenetic/metabolic processes and, for symbiotic species (4) the effect of symbionts. Our study verifies previously established slopes between $\Delta\delta^{13}C_{shell-DIC}$ and $[CO_3^{2-}]$ from laboratory culture experiments (Spero et al., 1997; Bijma et al., 1998, 1999). Because the $\Delta\delta^{13}C_{shell-DIC}/[CO_3^{2-}]$ slopes from our field data are similar to the ones established from culture experiments, we must conclude that there is no or little effect of temperature on the $\delta^{13}C_{shell-DIC}$. Despite a size-related ontogenetic/metabolic effect in $\delta^{13}C_{shell}$, the carbonate chemistry of surface waters thus appears to be an important mechanism controlling the carbon isotope composition in shells of planktic foraminifera. Most important, this study shows that in the NW Arabian Sea upwelling area, the carbonate ion effect and $\delta^{13}C_{DIC}$ act in an opposite sense on the shell's $\delta^{13}C$. On one hand, the ^{13}C depleted upwelled water lowers the shell's $\delta^{13}C$, while, on the other hand, the lower carbonate ion concentration (or lower pH) increases the shell's $\delta^{13}C$. Because both processes act in an opposite sense, the $\delta^{13}C$ in shells of planktic foraminifera reflect the net result of the changes in productivity (i.e. $\delta^{13}C_{DIC}$) and surface water carbonate chemistry.

5. Conclusions

In this study, we compared the distribution and stable isotope composition of shells of living *G. bulloides* and *G. ruber* to physical and chemical properties of the upper water column in the NW Arabian Sea. The following conclusions are drawn from this study.

(1) Shells of *G. bulloides* mirror upwelling conditions during the SW monsoon season. Shell concentrations of *G. bulloides* are two orders of magnitude higher during upwelling compared to the non-upwelling period. Shells of *G. ruber*, however, are produced during both monsoon seasons.

(2) During both monsoon seasons, the calcification temperature of *G. bulloides* and *G. ruber* mirror a depth level at or just below the deep chlorophyll maximum. Consequently, the average calcification temperature of *G. ruber* and *G. bulloides* is 1.7 ± 0.8 and 1.3 ± 0.9 °C lower than the sea surface temperature, respectively. Both species live at shallower depths during upwelling conditions than during non-upwelling periods.

(3) As a result of ontogenetic effects, large shells (250–355 μm) are enriched in ^{13}C by about 0.33 ± 0.15 ‰ (*G. bulloides*) and 0.39 ± 0.20 ‰ (*G. ruber*) compared to small ones (150–250 μm). The ontogenetic effect in the oxygen isotope composition between the two size fractions may be temperature dependent. On average, we found a difference of 0.23 ‰ (*G. bulloides*) and 0.17 ‰ (*G. ruber*) between the oxygen isotope composition of large and small shells.

(4) The $\delta^{13}C_{shell}$ values of *G. bulloides* and *G. ruber* are lower than the ambient $\delta^{13}C_{DIC}$. As a result of the carbonate chemistry in surface waters, the $\Delta\delta^{13}C_{shell-DIC}$ changes as a function of the carbonate ion concentration in seawater. The $\Delta\delta^{13}C_{shell-DIC}/[CO_3^{2-}]$ is species specific: for specimens in the 150–250 and 250–355 μm size fractions, we found $\Delta\delta^{13}C_{shell-DIC}/[CO_3^{2-}]$ slopes of -0.0066 ‰ and -0.0098 ‰ ($\mu mol\ kg^{-1}$) $^{-1}$ for *G. ruber*, and -0.012 ‰ and -0.013 ‰ ($\mu mol\ kg^{-1}$) $^{-1}$ for *G. bulloides*. These slopes compare well with results from laboratory culture experiments.

(5) The enigmatic carbon isotope composition of planktic foraminifera in the Arabian Sea upwelling areas, i.e. higher $\delta^{13}C_{shell}$ values during upwelling (lower $\delta^{13}C_{DIC}$), is largely the result of two processes that act in an opposite sense on the $\delta^{13}C$ of the shells: lower $\delta^{13}C_{DIC}$ values in upwelled waters lower the $\delta^{13}C_{shell}$, while the lower carbonate ion concentrations (or lower pH) in upwelled water result in an increase of the $\delta^{13}C_{shell}$.

(6) The $\Delta\delta^{18}O_{bul-rub}$ may be used as a proxy for seasonal surface water temperature variations.

Acknowledgements

The Netherlands Indian Ocean Programme was funded and coordinated by the Netherlands Marine Research Foundation (SOZ) of the Netherlands

Organization for Scientific Research (NWO). We thank Captain J. de Jong, technicians and crews of RV *Tyro*. We gratefully acknowledge Jan van Hinte, Susanne Lassen and Graham Mortyn for their comments and suggestions on a draft version of this manuscript. We thank Jelle Bijma and Howard Spero for reviewing this manuscript and for their valuable advice. Bryan Bemis is thanked for providing detailed information on his data. We thank Hubert Vonhof for his help with the mass-spectrometer. This is publication no. 3637 of the Netherlands Institute for Sea Research (NIOZ) and no. 20010903 of the Netherlands Research School of Sedimentary Geology.

References

- Anderson, D.M., Prell, W.L., 1993. A 300 kyr record of upwelling off Oman during the Late Quaternary: evidence of the Asian southwest monsoon. *Paleoceanography* 8, 193–208.
- Bé, A.W.H., 1967. Foraminifera families: *Globigerinidae* and *Globorotaliidae*. Fiches d'Identification du Zooplankton, sheet 108. Conseil Permanent International pour l'Exploration de la Mer, 1–3. Charlottenlund, Denmark.
- Bemis, B.E., Spero, H.J., Bijma, J., Lea, D., 1998. Reevaluation of the oxygen isotopic composition of planktonic foraminifera: experimental results and revised paleotemperature equations. *Paleoceanography* 13 (2), 150–160.
- Bemis, B.E., Spero, H.J., Lea, D.W., Bijma, J., 2000. Temperature influence on the carbon isotopic composition of *Orbulina universa* and *Globigerina bulloides* (planktic foraminifera). *Marine Micropaleontology* 38, 213–228.
- Berger, W.H., Killingley, J.S., Vincent, E., 1978. Stable isotopes in deep-sea carbonates: box core ERDC-92, west equatorial Pacific. *Oceanologica Acta* 1 (2), 203–216.
- Bijma, J., Hemleben, C., 1994. Population dynamics of the planktic foraminifer *Globigerinoides sacculifer* (Brady) from the central Red Sea. *Deep-Sea Research. Part I* 41, 485–510.
- Bijma, J., Spero, H.J., Lea, D.W., 1998. Oceanic carbonate chemistry and foraminiferal isotopes: new laboratory results, paper presented at the Sixth International Conference on Paleoceanography (I.C.P.), Lisbon, Portugal.
- Bijma, J., Spero, H.J., Lea, D.W., 1999. Reassessing foraminiferal stable isotope geochemistry: impact of the oceanic carbonate system (experimental results). In: Fischer, G., Wefer, G. (Eds.), *Use of Proxies in Paleoceanography: Examples from the South Atlantic*. Springer, Berlin, pp. 489–512.
- Bouvier-Soumagnac, Y., Duplessy, J.-C., 1985. Carbon and oxygen isotopic composition of planktonic foraminifera from laboratory culture, plankton tows and recent sediment: implications for the reconstruction of paleoclimatic conditions and of the global carbon cycle. *Journal of Foraminiferal Research* 15, 302–320.
- Brock, J.C., McClain, C.R., Anderson, D.M., Prell, W.L., Hay, W.W., 1992. Southwest monsoon circulation and environments of recent planktonic foraminifera in the northwestern Arabian sea. *Paleoceanography* 7, 799–813.
- Broecker, W.S., Peng, T.-H., 1982. Tracers in the Sea. Lamont-Doherty Geological Observatory, Columbia Univ., Palisades, NY 10964, 690 pp.
- Brummer, G.J.A., 1995. Plankton pump and multinet. In: Van Hinte, J.D., Van Weering, T.C.E., Troelstra, S.R. (Eds.), *Tracing a Seasonal Upwelling. Report on Two Cruises of RV Tyro to the NW Indian Ocean in 1992 and 1993*, vol. 4. National Museum of Natural History, Leiden, The Netherlands, pp. 31–40.
- Conan, S.M.-H., Brummer, G.-J., 2000. Fluxes of planktic foraminifera in response to monsoonal upwelling on the Somalia Basin margin. *Deep-Sea Research. Part 2* 47 (9–10), 2207–2227.
- Coplen, T.B., Kendall, C., Hopple, J., 1983. Comparison of stable isotope reference sample. *Nature* 302, 236–238.
- Craig, H., 1965. Measurements of oxygen isotope paleotemperatures. In: Tongiorgi, E. (Ed.), *Stable Isotopes in Oceanographic Studies and Paleotemperatures*. Cons. Naz. Ric., pp. 161–182. Spoleto, Italy.
- Craig, H., Gordon, L.I., 1965. Deuterium and oxygen 18 variations in the ocean and the marine atmosphere. In: Schink, D.R., Corless, J.T. (Eds.), *Stable Isotopes in Oceanographic Studies and Paleotemperatures*. Spoleto, July 26–27. Consiglio Nazionale delle Ricerche, Laboratorio di Geologia Nucleare, Pisa, pp. 9–130.
- Curry, W.B., Ostermann, D.R., Gupta, M.V.S., Ittekkot, V., 1992. Foraminiferal production and monsoonal upwelling in the Arabian Sea: evidence from sediment traps. In: Summerhays, C.P., Prell, W.L., Emeis, K.C. (Eds.), *Upwelling Systems: Evolution since the Early Miocene*. Geological Society Special Publication, vol. 64. The Geological Society, London, pp. 93–106.
- Delaygue, G., Bard, E., Rollion, C., Jouzel, J., Stievenard, M., Duplessy, J.-C., Ganssen, G., 2001. Oxygen isotope/salinity relationship in the northern Indian Ocean. *Journal of Geophysical Research* 106 (C3), 4565–4574.
- Deuser, W.G., Ross, E.H., Hemleben, C., Spindler, M., 1981. Seasonal changes in species composition, numbers, mass, size, and isotopic composition of planktonic foraminifera settling into the deep Sargasso Sea. *Palaeogeography, Palaeoclimatology, Palaeoecology* 33, 103–127.
- Dickson, A.G., 1990. Thermodynamics of the dissociation of boric acid in synthetic seawater from 273.15 to 318.15 K. *Deep-Sea Research* 37, 755–766.
- Duplessy, J.C., Bé, A.W.H., Blanc, P.L., 1981. Oxygen and carbon isotopic composition and biogeographic distribution of planktonic foraminifera in the Indian Ocean. *Palaeogeography, Palaeoclimatology, Palaeoecology* 33, 9–46.
- Epstein, S., Buchsbaum, R., Lowenstam, H.A., Urey, H.C., 1953. Revised carbonate-water isotopic temperature scale. *Bulletin of the Geological Society of America* 64, 1315–1326.
- Erez, J., Honjo, S., 1981. Comparison of isotopic composition of planktonic foraminifera in plankton tows, sediment traps and sediments. *Palaeogeography, Palaeoclimatology, Palaeoecology* 33, 129–156.
- Erez, J., Luz, B., 1983. Experimental paleotemperature equation for

- planktonic foraminifera. *Geochimica et Cosmochimica Acta* 47, 1025–1031.
- Fairbanks, R.G., Wiebe, P.H., 1980. Foraminifera and chlorophyll maximum: vertical distribution, seasonal succession, and paleoceanographic significance. *Science* 209, 1524–1526.
- Goyet, C., Coatanoan, C., Eiseheid, G., Amaoka, T., Okuda, K., Healy, R., Tsunogai, S., 1999. Spatial variation of total CO₂ and total alkalinity in the northern Indian Ocean: a novel approach for the quantification of anthropogenic CO₂ in seawater. *Journal of Marine Research* 57, 135–163.
- Guptha, M.V.S., Mohan, R.M., 1996. Seasonal variability of the vertical fluxes of *Globigerina bulloides* (d'Orbigny) in the northern Indian Ocean. *Mitteilungen aus dem Geologisch-Paläontologischen Institut der University Hamburg*, Heft 79, 1–17.
- Hemleben, C., Bijma, J., 1994. Foraminiferal population dynamics and stable carbon isotopes. In: Zahn, R., Pedersen, T.F., Kaminiski, M.A., Laberyrie, L. (Eds.), *Carbon Cycling in the Glacial Ocean: Constraints on the Ocean's Role in the Global Change-NATO ASI Series. Series I, Global Environmental Change*, vol. 17, pp. 145–166.
- Hemleben, C., Spindler, M., Anderson, O.R., 1989. *Modern Planktonic Foraminifera*. Springer, New York, 363 pp.
- Horibe, Y., Oba, T., 1972. Temperature scales of aragonite–water and calcite–water systems. *Paleontological Society of Japan* 23–24, 69–79.
- Hut, G., 1987. Stable isotope reference samples for geochemical and hydrological investigations. Consultants Group Meeting, 16–18.09.1985. International Atomic Energy Agency (I.A.E.A.), Vienna, Austria, 42 pp.
- Ithou, M., Ono, T., Oba, T., Noriki, S., 2001. Isotopic composition and morphology of living *Globorotalia scitula*: a new proxy of sub-intermediate ocean carbonate chemistry? *Marine Micropaleontology* 42, 189–210.
- Ivanova, E.M., 2000. Late Quaternary monsoon history and paleo-productivity of the western Arabian Sea. PhD thesis, Free University, Amsterdam, The Netherlands, 172 pp.
- Kahn, M.I., 1979. Non-equilibrium oxygen and carbon isotopic fractionation in tests of living planktonic foraminifera. *Oceanologica Acta* 2, 195–208.
- Kahn, M.I., Williams, D.F., 1981. Oxygen and carbon isotopic composition of living planktonic foraminifera from the Northern Pacific ocean. *Palaeogeography, Palaeoclimatology, Palaeoecology* 33, 47–69.
- Kim, S.-T., O'Neil, J.R., 1997. Equilibrium and non-equilibrium oxygen isotope effects in synthetic carbonates. *Geochimica et Cosmochimica Acta* 61, 3461–3475.
- Kohfeld, K.E., Fairbanks, R.G., Smith, S.L., Walsh, I.D., 1996. *Neogloboquadrina pachyderma* (sinistral coiling) as paleoceanographic tracers in polar oceans: evidence from Northeast Water Polynya plankton tows, sediment traps, and surface sediments. *Paleoceanography* 11 (6), 679–699.
- Körtzinger, A., Mintrop, L., Duinker, J.C., 1997. Strong CO₂ emissions from the Arabian Sea during South West Monsoon. *Geophysical Research Letters* 24, 1763–1766.
- Kroon, D., Darling, K., 1995. Size and upwelling control of the stable isotope composition of *Neogloboquadrina dutertrei* (D'Orbigny), *Globigerinoides ruber* (D'Orbigny) and *Globigerina bulloides* (D'Orbigny): examples from the Panama Basin and Arabian Sea. *Journal of Foraminiferal Research* 25, 39–52.
- Kroon, D., Ganssen, G., 1989. Northern Indian Ocean upwelling cells and the stable isotope composition of living planktonic foraminifera. *Deep-Sea Research* 36, 1219–1236.
- Kroon, D., Beets, K., Mowbray, S., Shimmield, G., Steens, T., 1990. Changes in northern Indian Ocean monsoonal wind activity during the last 500 ka. *Memorie della Societa Geologica Italiana* 44, 189–207.
- Kroopnick, P.M., 1985. The distributions of ¹³C of ΣCO₂ in the world ocean. *Deep-Sea Research* 32, 57–84.
- Lewis, E., Wallace, D.W.R., 1998. Program Developed for CO₂ System Calculations. ORNL/CDIAC-105. Carbon Dioxide Information Analysis Center, Oak Ridge National Laboratory, U.S. Department of Energy, Oak Ridge, Tennessee.
- McCreary, J.P., Kohler, K.E., Hood, R.R., Olson, D.B., 1996. A four-component ecosystem model of biological activity in the Arabian Sea. *Progress in Oceanography* 37, 193–240.
- Millero, F.J., 1979. The thermodynamics of the carbonate system in seawater. *Geochimica et Cosmochimica Acta* 43, 1651–1661.
- Millero, F.J., 1995. Thermodynamics of the carbon dioxide system in the oceans. *Geochimica et Cosmochimica Acta* 59, 661–677.
- Moos, C.A., 2000. Reconstruction of Upwelling Intensity and Paleo-nutrient Gradients in the Northwest Arabian Sea Derived from Stable Carbon and Oxygen Isotopes of Planktic Foraminifera. *Berichte aus dem Fachbereich Geowissenschaften der Universität Bremen* 156, 103 pp.
- Mulitza, S., Arz, H., Kemle-von Mücke, S., Moos, C., Niebler, H.-S., Pätzold, J., Segl, M., 1999. The South Atlantic carbon isotope record of planktic foraminifera. In: Fischer, G., Wefer, G. (Eds.), *Use of Proxies in Paleoceanography: Examples from the South Atlantic*. Springer, Berlin, pp. 427–445.
- Naidu, P.D., Malmgren, B.A., 1995. Monsoon upwelling effects on test size of some planktic foraminiferal species from the Oman margin, Arabian sea. *Paleoceanography* 10, 117–122.
- Naidu, P.D., Malmgren, B.A., 1996a. Relationship between Late Quaternary upwelling history and coiling properties of *N. pachyderma* and *G. bulloides* in the Arabian Sea. *Journal of Foraminiferal Research* 26, 64–70.
- Naidu, P.D., Malmgren, B.A., 1996b. A high-resolution record of late Quaternary upwelling along the Oman Margin, Arabian Sea based on planktonic foraminifera. *Paleoceanography* 11, 129–140.
- Niebler, H.-S., Hubberten, H.-W., Gersonde, R., 1999. Oxygen isotope values of planktic foraminifera: a tool for the reconstruction of surface water stratification. In: Fischer, G., Wefer, G. (Eds.), *Use of Proxies in Paleoceanography: Examples from the South Atlantic*. Springer, Berlin, pp. 165–189.
- Oppo, D.W., Fairbanks, R.G., 1989. Carbon isotope composition of tropical surface water during the past 22,000 years. *Paleoceanography* 4, 333–351.
- Peeters, F.J.C., 2000. The distribution and stable isotope composition of living planktic foraminifera in relation to seasonal changes in the Arabian Sea. Ph.D. Thesis, Free University, Amsterdam, The Netherlands, 184 pp.
- Peeters, F.J.C., Brummer, G.-J.A., in press. The seasonal and vertical distribution of living planktic foraminifera in the NW Ara-

- bian Sea. In: Clift, P., Kroon, D., Gaedicke, C., Craig, J. (Eds.), Tectonic and Climatic Evolution of the Arabian Sea Region. Geological Society Special Publication. Vol. 195. The Geological Society, London.
- Prell, W.L., Curry, W.B., 1981. Faunal and isotopic indices of monsoonal upwelling: western Arabian Sea. *Oceanologica Acta* 4, 91–98.
- Roy, R.N., Roy, L.N., Vogel, K.M., Porter-Moore, C., Pearson, T., Good, C.E., Millero, F.J., Campbell, D.M., 1993. The dissociation constants of carbonic acid in seawater at salinities 5 to 45 and temperatures 0 to 45 deg C. *Marine Chemistry* 44, 249–267.
- Russell, A.D., Spero, H.J., 2000. Field examination of the oceanic carbonate ion effect on stable isotopes in planktonic foraminifera. *Paleoceanography* 15 (1), 43–52.
- Shackleton, N.J., 1974. Attainment of isotopic equilibrium between ocean water and the benthonic foraminifera genus *Uvigerina*: isotopic changes in the ocean during the last glacial. *Centre National de la Recherche Scientifique, Colloques Internationaux* 219, 203–209.
- Shackleton, N.J., Vincent, E., 1978. Oxygen and carbon isotope studies in recent foraminifera from the southwest Indian Ocean. *Marine Micropaleontology* 3, 1–13.
- Spero, H.J., 1992. Do planktic foraminifera accurately record shifts in the carbon isotopic composition of sea water ΣCO_2 ? *Marine Micropaleontology* 19, 275–285.
- Spero, H.J., DeNiro, M., 1987. The influence of symbiont photosynthesis on the $\delta^{18}\text{O}$ and $\delta^{13}\text{C}$ values of planktonic foraminiferal shell calcite. *Symbiosis* 4, 213–228.
- Spero, H.J., Lea, D., 1996. Experimental determination of stable isotope variability in *Globigerina bulloides*: implications for paleoceanographic reconstructions. *Marine Micropaleontology* 28, 231–246.
- Spero, H.J., Williams, D.F., 1988. Extracting environmental information from planktonic foraminiferal $\delta^{13}\text{C}$ data. *Nature* 335, 717–719.
- Spero, H.J., Bijma, J., Lea, D.W., Bemis, B.E., 1997. Effect of seawater carbonate concentration on foraminiferal carbon and oxygen isotopes. *Nature* 390, 497–500.
- Steens, T.N.F., Ganssen, G., Kroon, D., 1992. Oxygen and carbon isotopes in planktic foraminifera as indicators of upwelling intensity and upwelling-induced high productivity in sediments from the north-western Arabian Sea. In: Summerhays, C.P., Prell, W.L., Emeis, K.C. (Eds.), *Upwelling Systems: Evolution since the Early Miocene*. Geological Society Special Publication, vol. 64. The Geological Society, London, pp. 107–119.
- Thunell, R., Sautter, L.R., 1992. Planktonic foraminiferal faunal and stable isotopic indices of upwelling: a sediment trap study in the San Pedro Basin, Southern California Bight. In: Summerhays, C.P., Prell, W.L., Emeis, K.C. (Eds.), *Upwelling Systems: Evolution since the Early Miocene*. Geological Society Special Publication, vol. 64. The Geological Society, London, pp. 77–91.
- Van Hinte, J.E., Van Weering, T.J.C.E., Troelstra, S.R., 1995. Tracing a seasonal upwelling. Report on two cruises of RV *Tyro* to the NW Indian Ocean in 1992 and 1993. National Museum of Natural History, Leiden, The Netherlands, 146 pp.
- Vénec-Peyré, M.-T., Caulet, J.-P., 2000. Paleoproductivity changes in the upwelling system of Socotra (Somali Basin, NW Indian Ocean) during the last 72,000 years: evidence from biological signatures. *Marine Micropaleontology* 40, 321–344.
- Weiss, R.F., 1974. Carbon dioxide in water and seawater: the solubility of a non-ideal gas. *Marine Chemistry* 2, 203–215.
- Williams, D.F., Sommer II, M.A., Bender, M.L., 1977. Carbon isotopic compositions of Recent planktonic foraminifera of the Indian Ocean. *Earth and Planetary Science Letters* 36, 391–403.
- Williams, D.F., Bé, A.W.H., Fairbanks, R.F., 1981. Seasonal stable isotopic variations in living planktonic foraminifera from Bermuda plankton tows. *Palaeogeography, Palaeoclimatology, Palaeoecology* 33, 71–102.
- Wyrki, K., 1971. *Oceanographic Atlas of the International Indian Ocean Expedition*. Publ. National Science Foundation-IDOE-1, Washington, DC, 531 pp.
- Wyrki, K., 1988. *Oceanographic Atlas of the International Indian Ocean Expedition*. Amerind Publishing, New Delhi, 531 pp.
- Zeebe, R., 1999. An explanation of the effect of seawater carbonate concentration on foraminiferal oxygen isotopes. *Geochimica et Cosmochimica Acta* 63 (13/14), 2001–2007.